



This document was prepared for the ETI by third parties under contract to the ETI. The ETI is making these documents and data available to the public to inform the debate on low carbon energy innovation and deployment.

**Programme Area:** Marine

**Project:** PerAWAT

**Title:** Report of Calibrated Numerical Models of Anglesey and the Bristol Channel, including Validation Against Measured Data

### Abstract:

A two-dimensional depth-averaged numerical model of the United Kingdom and Irish coasts has been constructed that includes the Anglesey and the Bristol Channel regions. The model has been developed using the discontinuous Galerkin method based ADCIRC model (DG-ADCIRC). Bathymetric data are obtained from SeaZone and the tidal forcing data are taken from the Le Provost tidal database. Model results are compared to the available measurements. Bearing in mind the scale of the region being modelled, a very good agreement is achieved between model predictions and measured data. The model presented in this report is capable of capturing the general hydrodynamic response to the main tidal forcing constituents. Several discrepancies occur between the model predictions and field data at individual observation stations.

### Context:

The Performance Assessment of Wave and Tidal Array Systems (PerAWaT) project, launched in October 2009 with £8m of ETI investment. The project delivered validated, commercial software tools capable of significantly reducing the levels of uncertainty associated with predicting the energy yield of major wave and tidal stream energy arrays. It also produced information that will help reduce commercial risk of future large scale wave and tidal array developments.

### Disclaimer:

The Energy Technologies Institute is making this document available to use under the Energy Technologies Institute Open Licence for Materials. Please refer to the Energy Technologies Institute website for the terms and conditions of this licence. The Information is licensed 'as is' and the Energy Technologies Institute excludes all representations, warranties, obligations and liabilities in relation to the Information to the maximum extent permitted by law. The Energy Technologies Institute is not liable for any errors or omissions in the Information and shall not be liable for any loss, injury or damage of any kind caused by its use. This exclusion of liability includes, but is not limited to, any direct, indirect, special, incidental, consequential, punitive, or exemplary damages in each case such as loss of revenue, data, anticipated profits, and lost business. The Energy Technologies Institute does not guarantee the continued supply of the Information. Notwithstanding any statement to the contrary contained on the face of this document, the Energy Technologies Institute confirms that the authors of the document have consented to its publication by the Energy Technologies Institute.



## Energy Technologies Institute

### PerAWaT

# WG3 WP6 D4B — REPORT OF CALIBRATED NUMERICAL MODELS OF ANGLESEY AND THE BRISTOL CHANNEL, INCLUDING VALIDATION AGAINST MEASURED DATA

**Authors** S. Serhadlioglu, T.A.A. Adcock,  
G.T. Houlsby, and A.G.L. Borthwick

**Version** 2.0

**Date** 27/3/2012

Revision History		
Issue / Version	Issue Date	Summary
0.1	16/03/2012	Preliminary report submitted to GH.
1.0	19/03/2012	Report submitted to GH.
2.0	27/03/2012	Corrected report submitted to GH.

## ***Executive Summary***

A two-dimensional depth-averaged numerical model of the United Kingdom and Irish coasts has been constructed that includes the Anglesey and the Bristol Channel regions. The model has been developed using the discontinuous Galerkin method based ADCIRC model (DG-ADCIRC). Bathymetric data are obtained from SeaZone and the tidal forcing data are taken from the le Provost tidal database. Model results are compared to the available measurements. Bearing in mind the scale of the region being modelled, a very good agreement is achieved between model predictions and measured data. The model presented in this report is capable of capturing the general hydrodynamic response to the main tidal forcing constituents. Several discrepancies occur between the model predictions and field data at individual observation stations. The reasons are being investigated, and we anticipate further fine-tuning of the model to be presented in WG3 WP6 D6.

## Contents

<b>Executive Summary .....</b>	<b>2</b>
<b>1. Acceptance Criteria .....</b>	<b>4</b>
<b>2. Model Set-up and Parameters .....</b>	<b>5</b>
2.1 Introduction .....	5
2.2 Computational Mesh.....	7
2.3 Boundary Conditions.....	9
2.4 Model Parameters.....	12
<b>3. Model Results.....</b>	<b>15</b>
3.1 Tidal Harmonics .....	15
3.2 The Bristol Channel.....	24
3.3 Anglesey .....	37
<b>Conclusions .....</b>	<b>49</b>
<b>References .....</b>	<b>50</b>
<b>Appendix 1: Bathymetry data .....</b>	<b>52</b>

## 1. Acceptance Criteria

Acceptance criteria for this deliverable are set out in Table 1.

Acceptance criteria	Location in report
Report describes:  a. calibration methodology b. quantifies model performance of key parameters including errors and sensitivities against observations: <ul style="list-style-type: none"><li>- Water surface elevations</li><li>- Currents</li></ul>	  a. Section 2: Model Set-up and Parameters, p: 5-15 b. Section 3: Model Results, p: 15-49
Input files in format to be agreed	Input files are attached separately

**Table 1 Acceptance criteria**

### ***Required Input Files***

As detailed in WG3 WP6 D4A, the input file “fort.14” includes the proprietary bathymetric data from SeaZone and, due to the licensing restrictions on use of these data, the bathymetric data in the “fort.14” file has been replaced with public domain, freely available data obtained from GEBCO. The format of the input files can be summarised as below,

- 1) fort.14: This input file has three parts. The first consists of the coordinates and bathymetric depth of each computational node, the second details the triangulation of the nodes and the third details the boundary conditions.
- 2) fort.15: This file specifies various attributes where model parameters can be changed by users.
- 3) fort.dg: This file specifies the function and other details to be used regarding the discontinuous Galerkin solution.

The tidal forcing data are specified in the “fort.15” file. The model simulation is arbitrarily set to start on 1<sup>st</sup> January 2012. The simulations are run for 29 days including one day for the “spin-up” period. The spin-up period is the time required for the model to remove the effects of the initial conditions and to reach a stable solution.

## ***2. Model Set-up and Parameters***

### **2.1 Introduction**

WG3 WP6 D4 involves the creation of two-dimensional shallow water models of selected tidal basins around the United Kingdom. The chosen sites are the Pentland Firth, the Anglesey Skerries and the Bristol Channel. The reasoning behind the selection of these sites is given in WG3 WP6 D3, and is therefore not be repeated in this report. The validated two-dimensional depth-averaged model for the Pentland Firth site is reported in WG3 WP6 D4A. The numerical modelling of the other two regions is presented in this report. Originally, it was anticipated that two separate models would be created for the Bristol Channel and Anglesey regions. However, early research indicated that these sites are sufficiently close that there may be significant hydrodynamic interaction, and furthermore that two individual models would involve a considerable area of overlap. It has therefore been decided to construct a single comprehensive model that covers the two sites. An advantage of this combined model is that interactions between the two sites may be specifically addressed. The disadvantage of the single larger model is that it makes higher computational demands. However, on balance it was considered that the advantages of the combined model outweigh the difficulties. Figure 1 shows the domain of the numerical model developed.

There are three important outer “forcing” boundaries for the model. The first is the boundary with the Atlantic to the southwest. This boundary is set just beyond the continental shelf, as this robustly models the tidal forcing (Adcock, 2011). There is a minor forcing boundary at the western end of the English

Channel, positioned to avoid having to model the Channel in detail. A small (and highly simplified) section of the French coast in the vicinity of Cape Finisterre is included. This allows the flux to and from the English Channel to be cleanly separated in the model from other fluxes. Finally there is a small forcing boundary representing the North Channel between Ulster and Galloway.



**Figure 1 The domain included in the numerical model shown by dashed red lines (Google Earth, 2012)**

As explained in WG3 WP6 D4A, modelling of a large domain is computationally demanding and requires a pragmatic approach with regard to mesh resolution. The finer the mesh resolution, the smaller is the time step required in order to satisfy stability criteria [such as the Courant-Friedrichs-Lewy (CFL) condition, which is of importance as an explicit time discretisation is used]. There is a balance to be struck between resolution and computational performance. This report describes the development of a model at a resolution that captures the

dominant hydrodynamic responses of the basins to the tides. Criteria outlined in WG3 WP6 D4A are adopted for islands located in the model.

## **2.2 Computational Mesh**

In order to create the computational mesh, the coastline of the region to be modelled has been determined from bathymetric contour data, which is obtained from SeaZone. The data were provided in “shapefile” format, which was read in the meshing software SMS using the GIS module function. The shapefiles consist of mean sea level (MSL) and intertidal level contour data. The MSL contour data have been used to construct the model for the areas of interest. Meshing was then carried out using SMS. Several manual corrections have been made to the resulting mesh in order to improve its quality. The mesh size varies between 200 m (around the islands in the Bristol Channel and Anglesey) and 50 km (close to the continental shelf on the southern boundary). The resolution of the mesh in the Bristol Channel region is around 1 km, whereas in the Anglesey region it is 1.5 km. The total number of elements in the mesh is 25841. Considering that Anglesey and the Bristol Channel are located fairly close to each other, the model is intended to capture the interactions between these two sites, when tidal turbines are installed in both of these regions. A single unstructured triangular finite element mesh has been constructed that has boundaries ranging from the North Channel to southern continental shelf (Figure 2). The southwestern and southern boundaries of the mesh reach towards the continental shelf to capture the quarter wavelength resonance occurring in the Bristol Channel. The southeastern boundary is located from the Lizard in Cornwall to the tip of Brittany. Figure 3 and Figure 4 provide snapshots of the mesh in the Bristol Channel and Anglesey. As part of this deliverable the mesh information is supplied electronically in the form of fort.14 file.



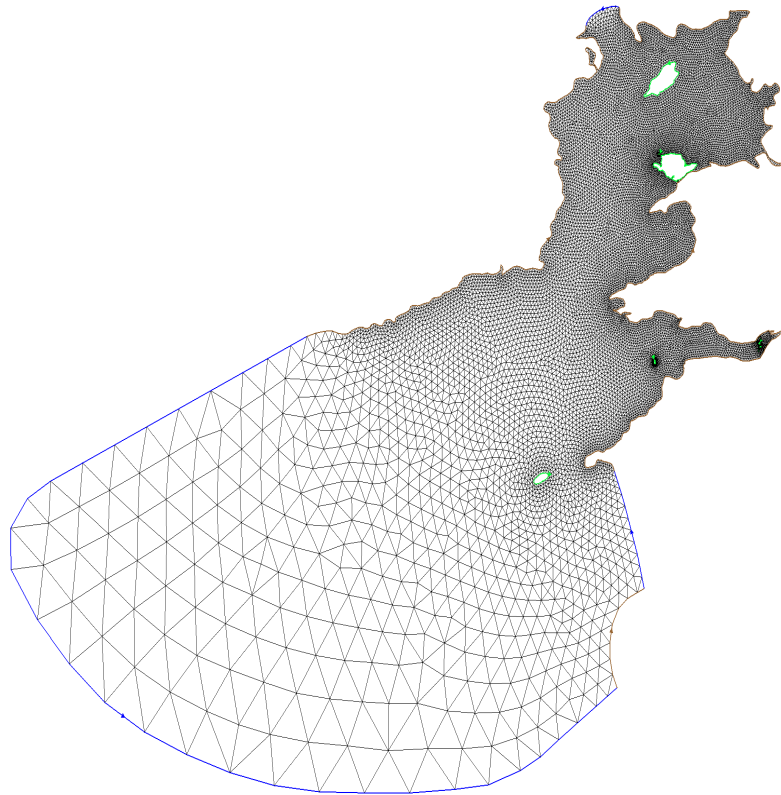


**Figure 2 Mesh used for the combined model of Anglesey and the Bristol Channel**

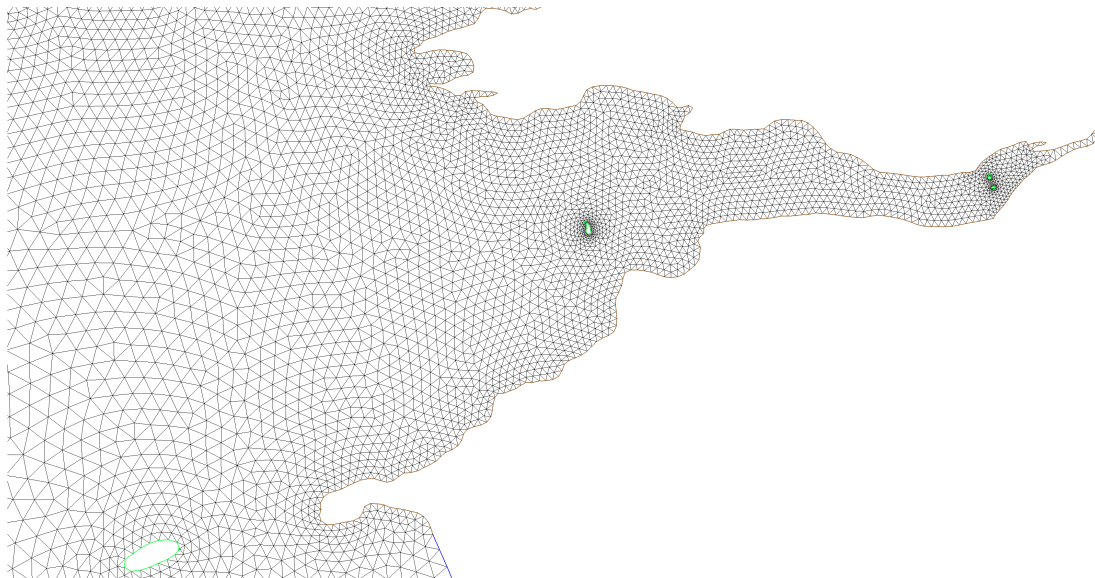


**Figure 3 Detail of mesh around the Bristol Channel**

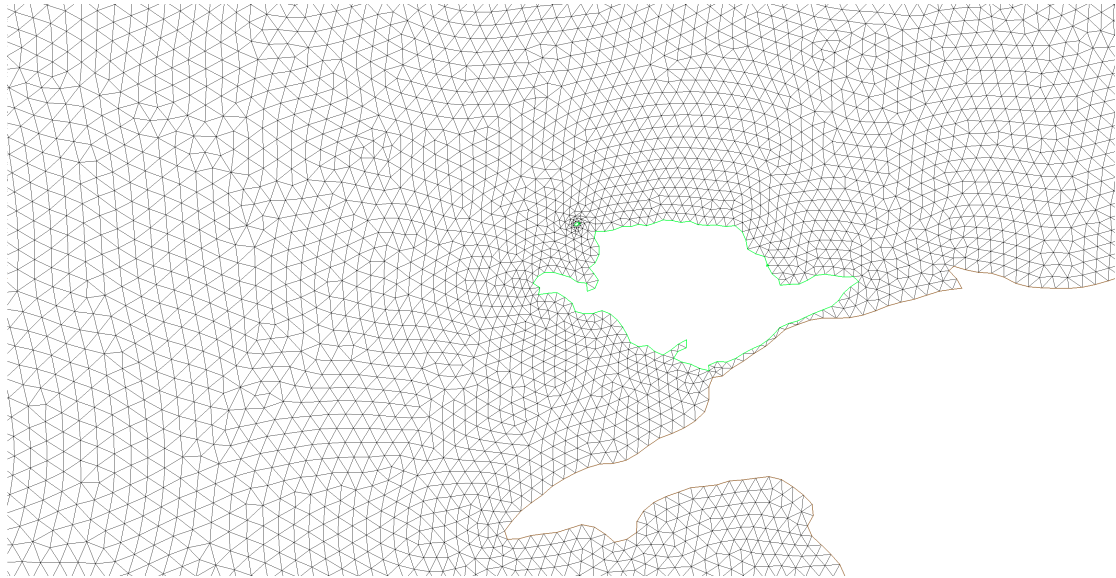


**Figure 4 Detail of mesh around Anglesey**

## **2.3 Boundary Conditions**

### ***Bathymetry***

WG3 WP6 D3 provides details about the bathymetric data purchased from SeaZone. Figure 5 shows a visualization of the bathymetry obtained using the SeaZone data [interpolated from high resolution (20 m) and high quality data (survey dataset) for the Bristol Channel and Anglesey regions, and from lower quality data (charted dataset) for the remainder of the domain]. Appendix 1 lists the set of files used in the model. The datum of the charted dataset has been altered so that all datasets are referred to a consistent mean sea level (MSL). The onward use of the SeaZone data is limited by proprietary restrictions, and so the SeaZone data have been replaced by freely available data from GEBCO (Monahan, 2008). Figure 6 shows the computational mesh interpolated from the GEBCO data. Note, however, that in some regions the lower quality GEBCO data led to somewhat unrealistic features in the bathymetry. As argued in WG3 WP6 D3 these inaccuracies have required us to purchase higher resolution data.

Modelling coastal basins that include intertidal zones would require a special treatment in the solution. For instance, the intertidal zone would be inundated

during a flood tide and dried out during an ebb tide. This moving boundary problem seen in shallow water models is referred as the wetting and drying problem (Bunya *et al.*, 2009). The wetting and drying treatment is computationally an expensive feature, and so in this model, it is not included in the analysis. In order to prevent any instability that might occur due to the elements that would otherwise dry out, the coastline for the model mesh has been interpolated with a mean sea level of 6.0 m (the approximate largest half amplitude of the tide). It is anticipated that the influence of wetting and drying will be explored later for the Bristol Channel area, as it is possible that it may influence the results. The analysis will be reported in WG3 WP6 D6.

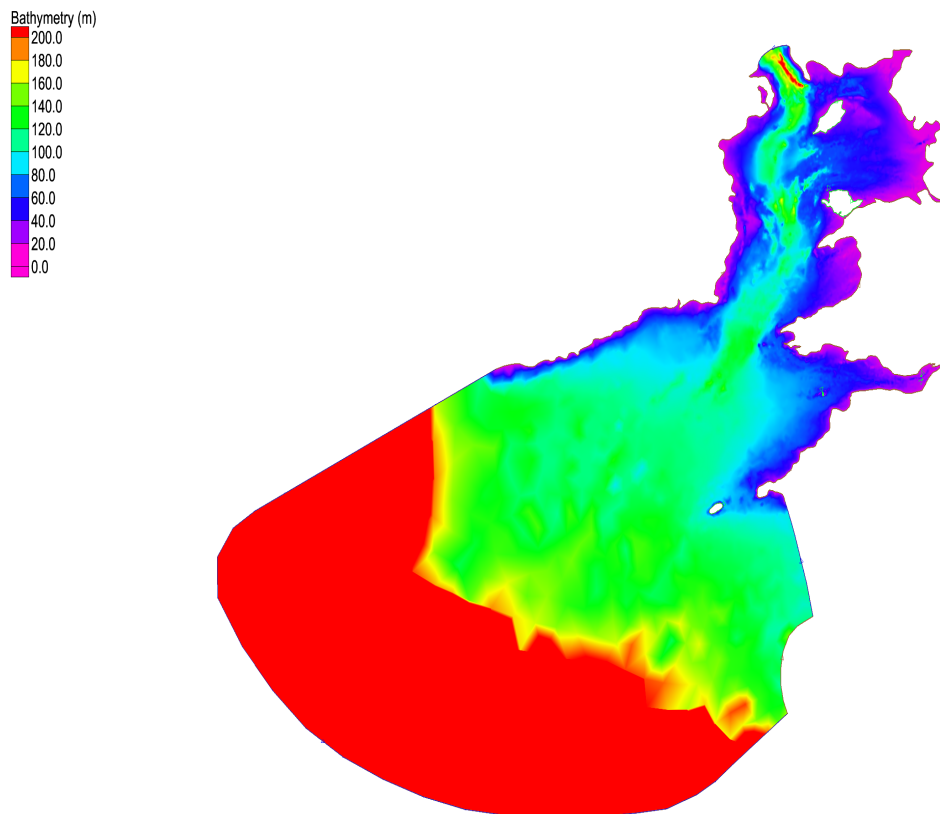


**Figure 5 Bathymetry of the numerical model obtained by using SeaZone data.**

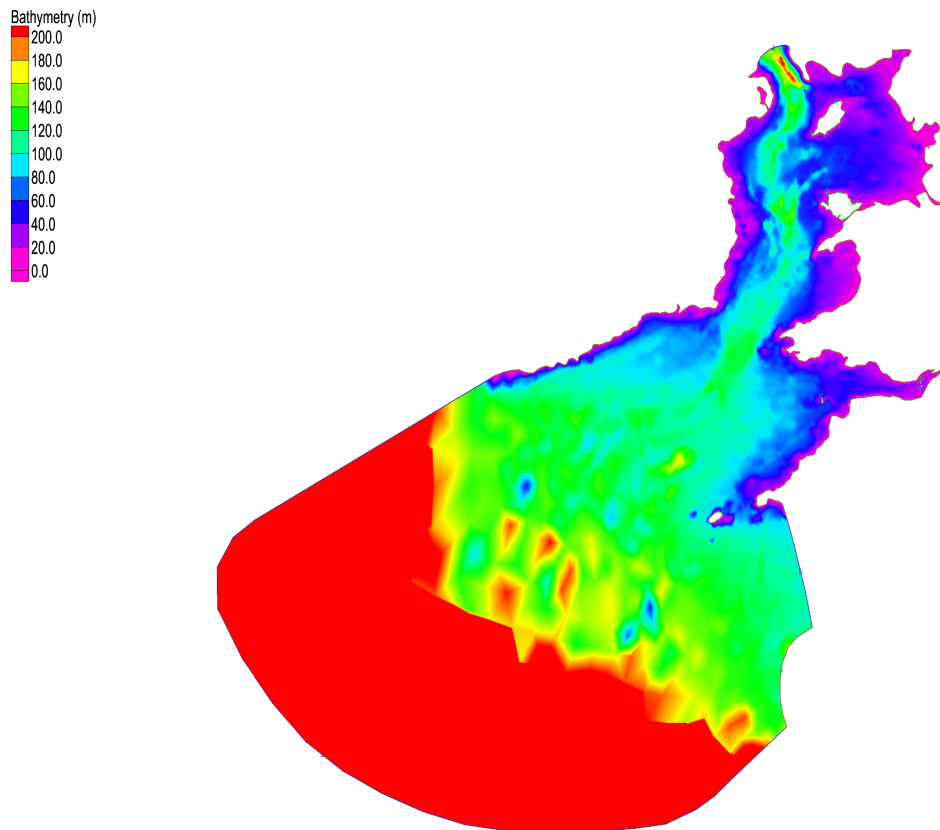


**Figure 6 Bathymetry of the numerical model obtained by using GEBCO data.**

### ***Tidal Forcing***

In basin scale modelling, the coastal domain is truncated through the use of artificial (open) boundaries that separate the area of interest from a connecting body of water. These open boundaries are forced by tidal flows of specified free surface and/or flux time histories. Following the arguments given in WG3 WP6 D3, the open boundaries of the present numerical model are forced by specifying the amplitude and phases of prescribed tidal constituents. In practice, these forcing parameters can be obtained from various tidal databases, which use low-resolution models to compute the tidal amplitudes and phases around the world. These values are then interpolated onto the open boundaries of the computational domain. Herein, the Le Provost tidal database (Le Provost et al., 1995) is used to force the model utilised in the present deliverable. The reasoning behind this selection is given in WG3 WP6 D3. Figure 7 indicates the mesh covered by the Le Provost database that includes data on 13 principal tidal

constituents ( $2N_2$ ,  $K_1$ ,  $K_2$ ,  $L_2$ ,  $M_2$ ,  $MU_2$ ,  $N_2$ ,  $NU_2$ ,  $O_1$ ,  $P_1$ ,  $Q_1$ ,  $S_2$ ,  $T_2$ ). For both locations considered, the tide is dominated by the  $M_2$  and  $S_2$  components (approximately 95% of the total tidal amplitude). Thus the model developed for the present deliverable is forced by the two main semi-diurnal tidal components,  $M_2$  and  $S_2$ .

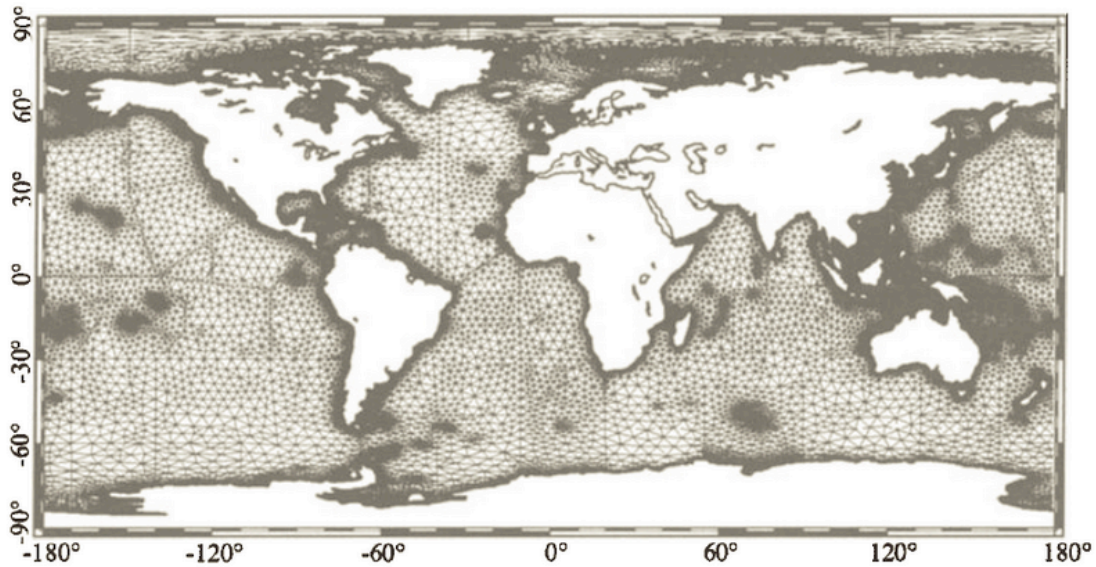


**Figure 7 The LeProvost tidal database coverage, (Le Provost et al., 1995)**

As power is approximately related to the magnitude cubed, it is reasonable to neglect the remaining smaller components in energy resource assessment. Although higher-harmonic  $M_4$  and  $M_6$  components related to local bed friction and bed topography are not introduced at the open boundaries, their effects are nevertheless captured within the model and can be investigated through tidal harmonic analysis of the model outputs. It is straightforward to include additional tidal components in the forcing model if that is deemed necessary.

## **2.4 Model Parameters**

Table 2 and Table 3 list the parameters used for the model. Table 2 relates to the “fort.15” file, whereas Table 3 gives information on the functions required for a discontinuous Galerkin solution. Several parameters used in Table 2 are

obtained through numerical experimentation as part of the calibration process (in particular the bed friction coefficient).

<b>Parameter</b>	<b>Value</b>	<b>Notes</b>
Time-step	0.5 s	To ensure stability, the time-step must satisfy the CFL condition, and diffusivity criteria, and so is dependent on the finest mesh size and the polynomial order used.
Ramping duration	1 day	To avoid shock-waves developing in the computation
Simulation period	29 days	At least 28 days is required for harmonic analysis <sup>1</sup>
Eddy viscosity coefficient	2 m <sup>2</sup> /s	Average value adopted for basin-scale hydrodynamic models
Non-linear bed friction coefficient	0.005	In the computations, the amplitudes have not been found to significantly on this parameter, although further fine-tuning may be appropriate
Coriolis Force	Automatic	Derived from latitude and longitude
Harmonics used	M <sub>2</sub> , S <sub>2</sub>	Most significant components in the area
Wetting and drying	Off	See the discussion below

**Table 2 Parameters used in final model run**

---

<sup>1</sup> A sensitivity test has been conducted regarding the spin-up period time. A spin-up period of one day results in large signal to noise ratio in the harmonic analysis and hence is considered sufficient.

Parameter	Value	Notes
Polynomial Order	1 <sup>st</sup> order	A piecewise linear approximation is used in the computation
Flux type	Local Lax Friedrichs (LLF)	Robust scheme for large domains involving regions with low flow velocities (Tu and Aliabadi, 2005)
SSP-Runge Kutta time stepping stage and order	2, 2	Standard values for linear elements (Kubatko <i>et al.</i> , 2008)

**Table 3 Parameters used for the discontinuous Galerkin solution**

There are significant regions in the Bristol Channel and in the estuaries on the east side of the Irish Sea where wetting and drying occurs during the tidal cycle. However, the inclusion of wetting and drying requires very much longer run times, so it should only be used when absolutely necessary. As will be seen below, the calibration of the current model (without wetting and drying) achieves a very good match to the conditions in this region, and so the model would provide an entirely satisfactory basis within which to study the incremental effects of tidal energy extraction. However, if maximum accuracy is to be achieved at specific sites (as may be required by future developers) it may be necessary to include wetting and drying. For the purposes of this project, we anticipate that it will not be necessary to introduce wetting and drying for the study of the Anglesey site. However, the detailed modelling of tidal energy extraction in the Bristol Channel will include examination of the effects of inclusion of wetting and drying in the analysis.

### **3. Model Results**

The present deliverable is a validated two-dimensional depth-averaged numerical model that simulates tidal dynamics at selected coastal sites off the United Kingdom. Model validation is undertaken against observed data, obtained from the Admiralty's Total Tide software and BODC current data, for the Bristol Channel and Anglesey regions. The validation study also includes a tidal harmonic analysis comparison against predictions by alternative numerical models (Davies and Jones, 1992; Robinson, 1978). Section 3.1 describes the harmonic analysis undertaken for  $M_2$  and  $S_2$  tidal constituents for the whole computational domain. Section 3.2 focuses on surface elevations and current velocities in the Bristol Channel. Section 3.3 considers the Anglesey region.

#### **3.1 Tidal Harmonics**

Tidal analyses are used to predict future tides from observed sea level and current data and to understand the hydrodynamic response of the sea to tidal forcing (Pugh, 1987). In the latter case, tidal analysis can be used to represent the tidal characteristics of a designated region. Harmonic analysis involves a Fourier decomposition of observed tidal data obtained over a time period into a finite number of harmonic constituents whose amplitude and phases relate to different astronomical parameters (Doodson, 1921). Each harmonic constituent is represented by (see e.g. Pugh, 1987),

$$H_n \cos(\sigma_n t - \varphi_n) \tag{3.1}$$

where,  $H_n$  is the amplitude,  $\sigma_n$  is the angular speed (frequency),  $\varphi_n$  is the phase lag of the tidal constituent, and  $t$  is time. In the present work, the numerical model is forced by specifying interpolated semi-diurnal  $M_2$  and  $S_2$  constituents on the open boundaries. The results are then compared against co-tidal maps provided by Davies and Jones (1992). Figure 8 shows the co-tidal contours of  $M_2$  amplitude; Figure 9 presents the phase of  $M_2$  in degrees. Figure 10 presents results for  $M_2$  constituent obtained by Davies and Jones (1992) using an alternative numerical model.



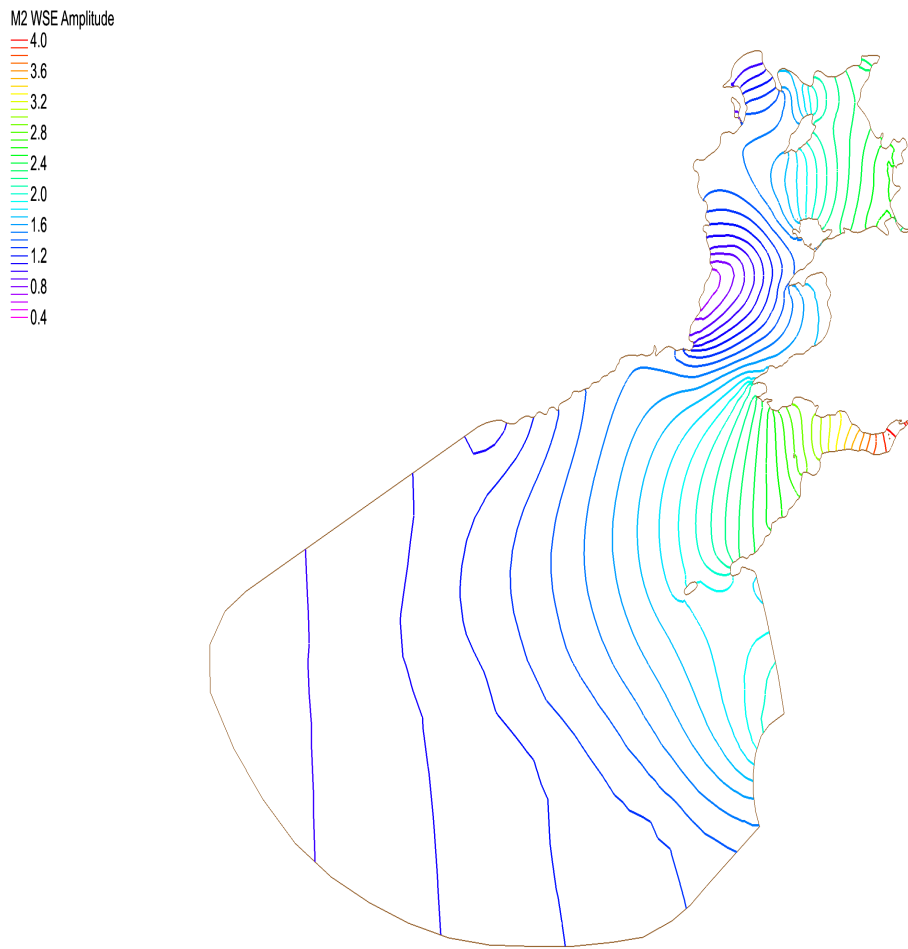


**Figure 8 Computed  $M_2$  co-tidal amplitude contours (m) using DG-ADCIRC.**

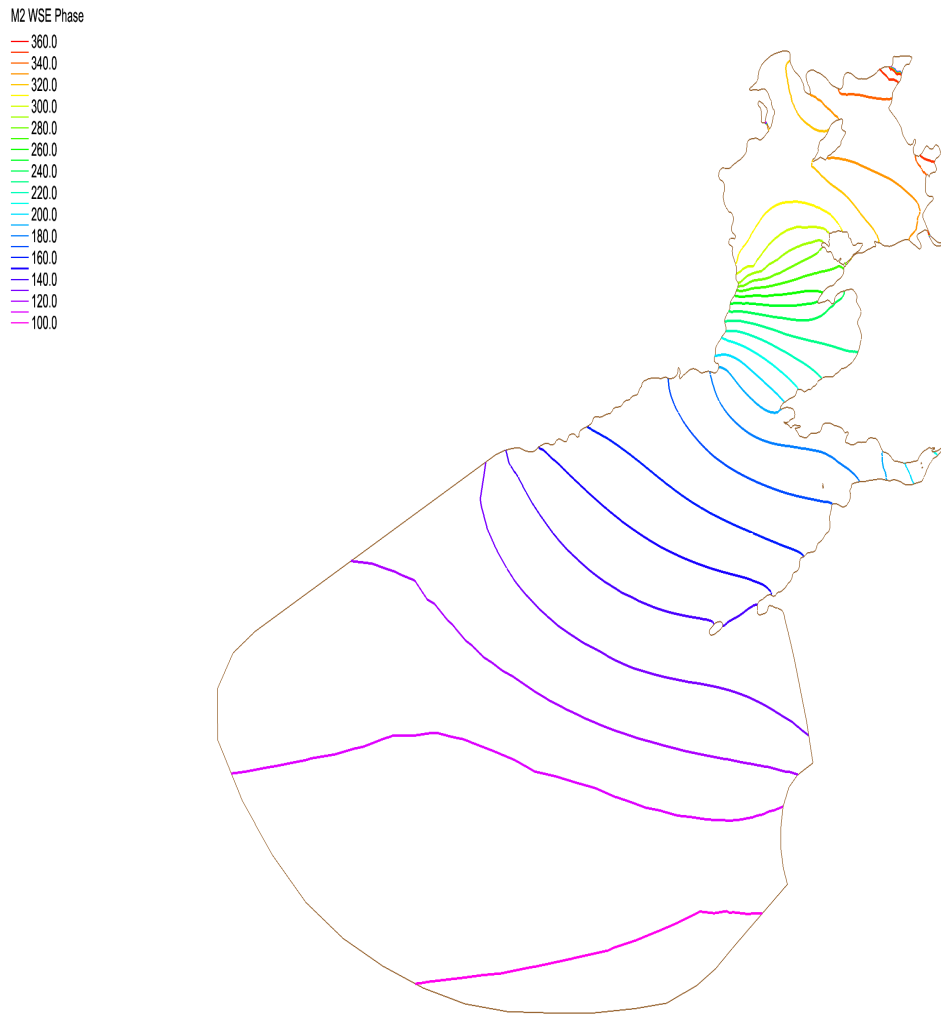


**Figure 9 Computed  $M_2$  co-tidal phase contours (degrees) using DG-ADCIRC.**

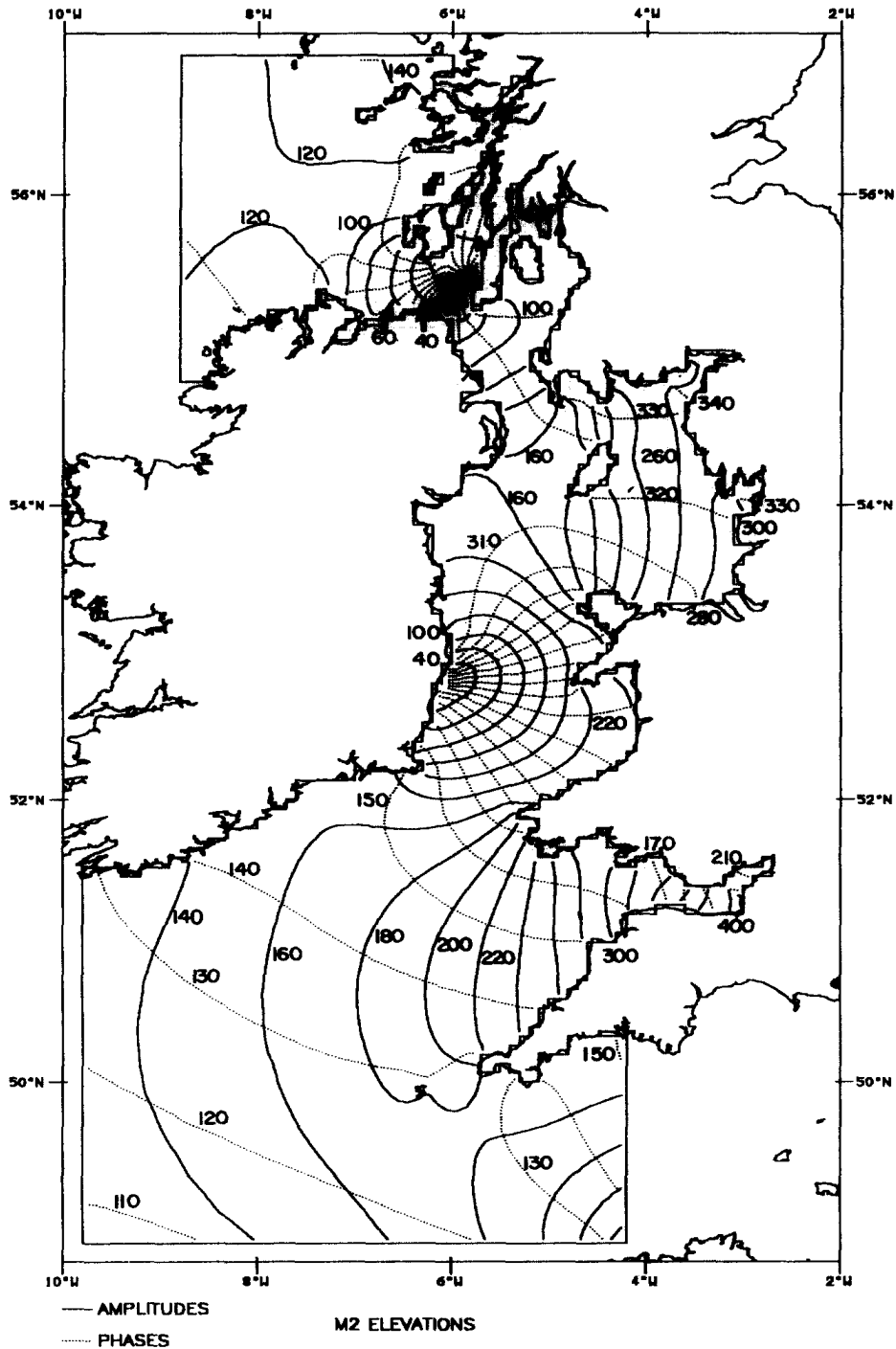
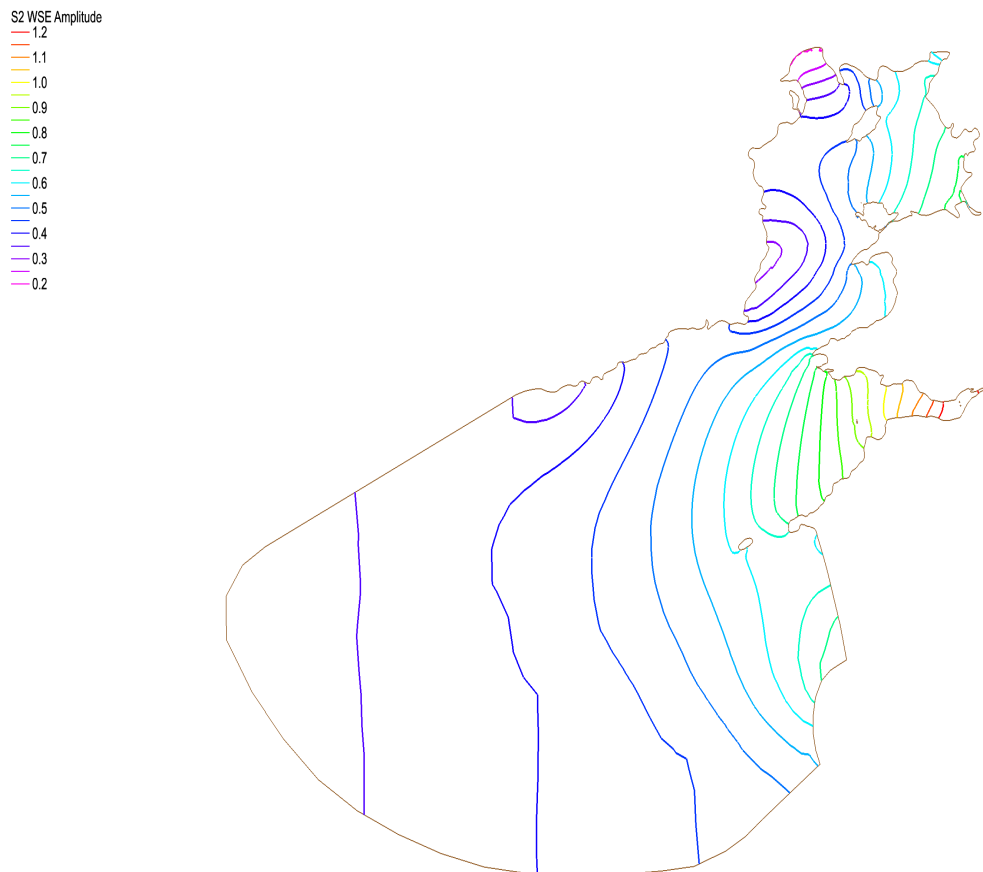


Figure 10 Computed  $M_2$  co-tidal chart obtained by Davies and Jones (1992). Solid lines = amplitudes in cm; dashed lines = phases in degrees.

The model results (Figure 8 and Figure 9) for  $M_2$  co-tidal charts are in excellent visual agreement with charts presented by Davies and Jones, 1992 (Figure 10) and Robinson (1978). The present model reproduces the “amphidromic point”

generated off the east coast of Ireland. An amphidromic point occurs in a region where the amplitude of a harmonic constituent tends to zero, implying no change in water level of the tidal cycle. Phase lines emanate from these amphidromic points about which the tidal wave circulates. The model results show that both the  $M_2$  and  $S_2$  tidal amplitudes increase considerably from Milford Haven to Avonmouth within the Bristol Channel. The  $M_2$  tidal amplitude is also amplified in the Irish Sea basin near the northwest Lancashire and Cumbrian coastline of the U.K. Figure 11 and Figure 12 show the computed  $S_2$  co-tidal charts for amplitude (m) and phase (degrees) respectively. The DG-ADCIRC model predictions show a close visual agreement with the results presented by Davis and Jones (1993) shown in Figure 13. Both sets of semi-diurnal constituents are similar, and include the amphidrome for the  $S_2$  constituent.



**Figure 11  $S_2$  co-tidal amplitude (m) contours predicted using DG-ADCIRC.**

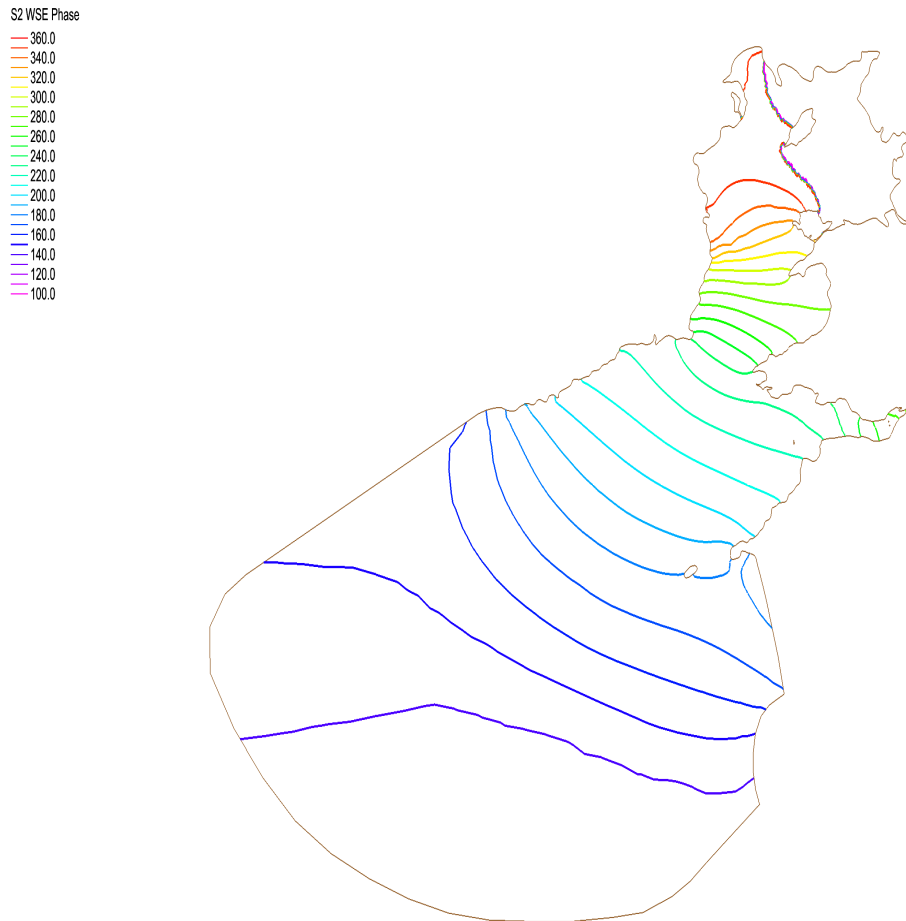


**Figure 12 S<sub>2</sub> co-tidal phase contours (degrees) predicted by DG-ADCIRC.**

In a study of tidal dynamics observed in the Irish Sea, Howarth (1984) reports that the semi-diurnal tides propagate into the Irish Sea both from the south (through the Celtic Sea) and from the north (the North Channel). Those two waves interfere with each other in the vicinity of the Isle of Man and are then reflected by the Lancashire and Cumbrian coasts. This interaction forms a standing wave in the eastern Irish Sea, which translates into high tidal amplitudes that rapidly develop throughout the eastern Irish Sea. This explains the rapid phase difference evident in the S<sub>2</sub> tidal constituent in Figure 12.

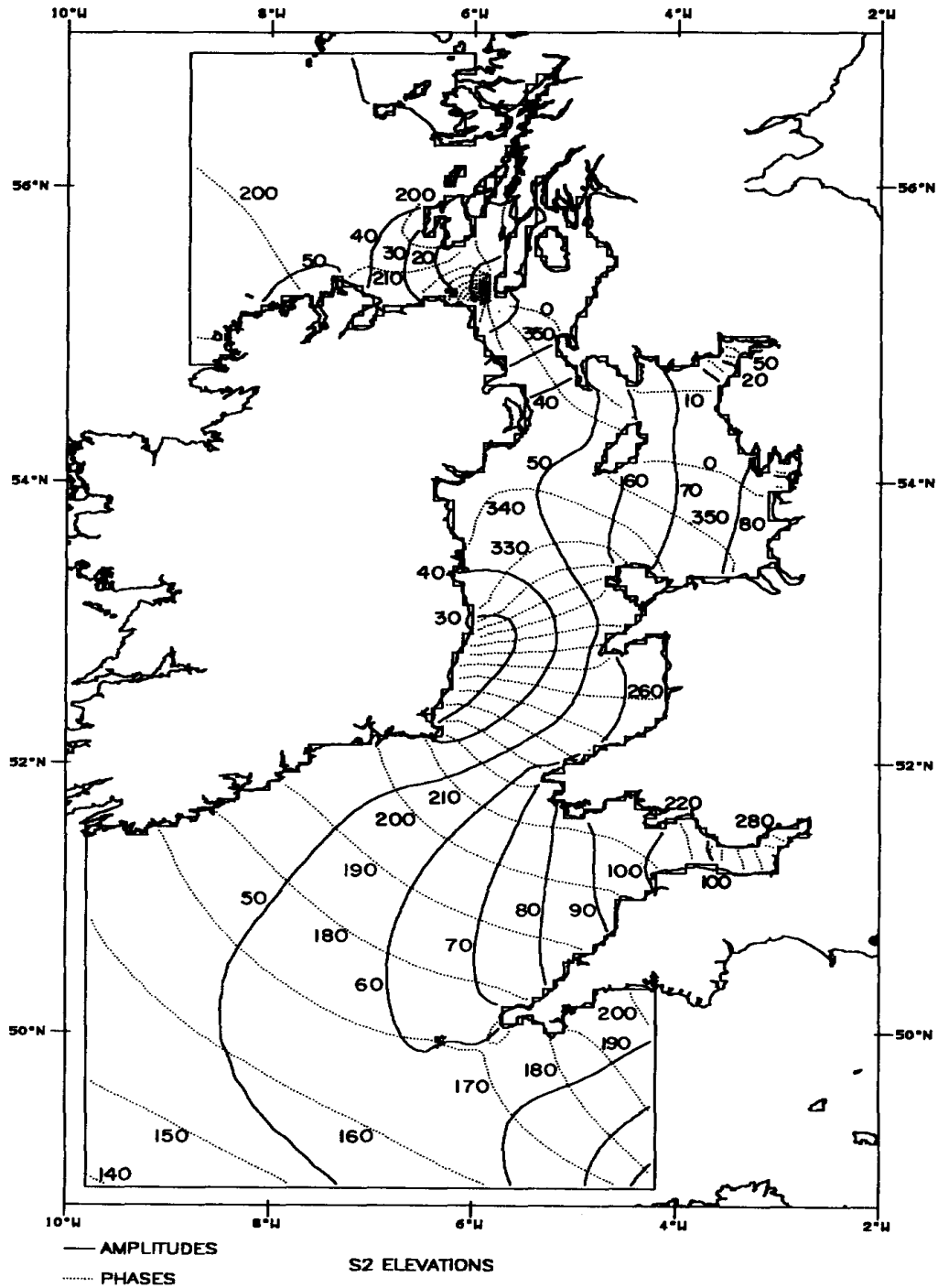
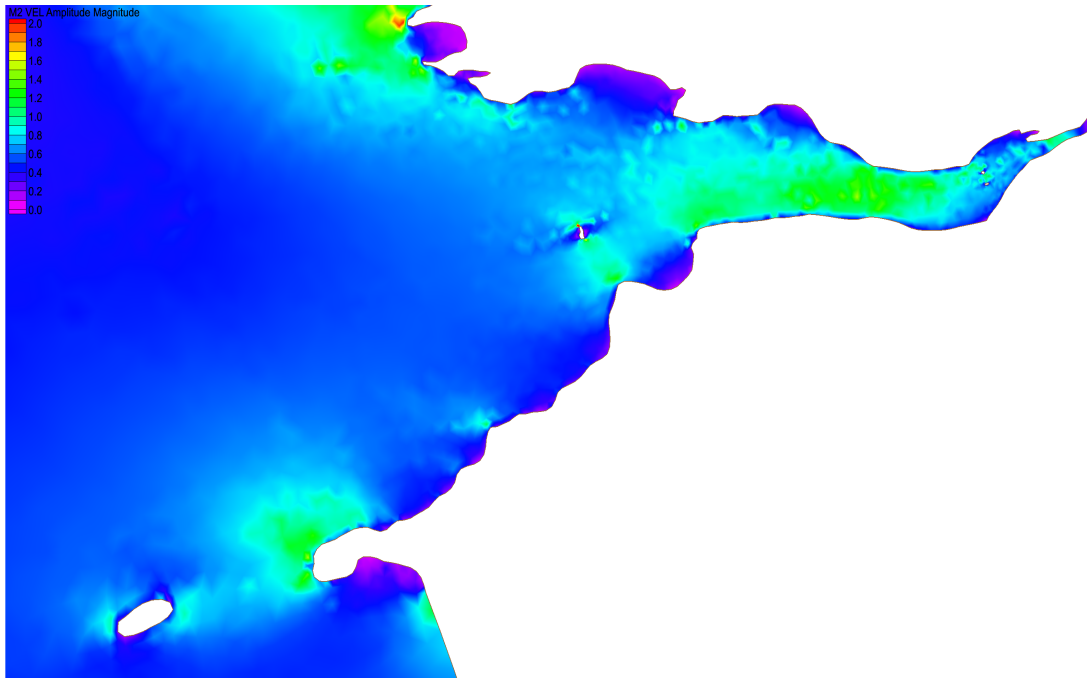


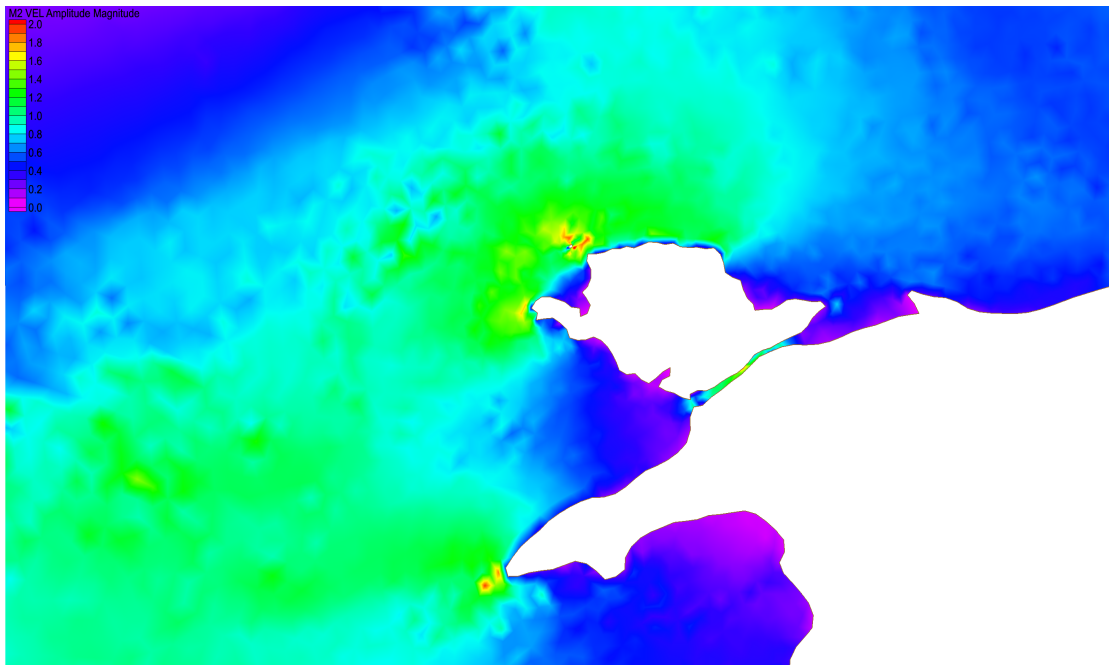
Figure 13 S<sub>2</sub> co-tidal chart computed by Davies and Jones (1992). Solid lines = amplitudes (cm); dashed lines = phases (degrees).

Figure 14 and Figure 15 present the predicted M<sub>2</sub> tidal current magnitudes for the Bristol Channel and Anglesey regions, using ADCIRC's tidal harmonic analysis

function. Figure 16 and Figure 17 present the corresponding  $S_2$  tidal current magnitudes.



**Figure 14  $M_2$  tidal current amplitude in the Bristol Channel region (m/s) predicted by DG-ADCIRC.**



**Figure 15  $M_2$  tidal current amplitude in the Anglesey region (m/s) predicted by DG-ADCIRC.**

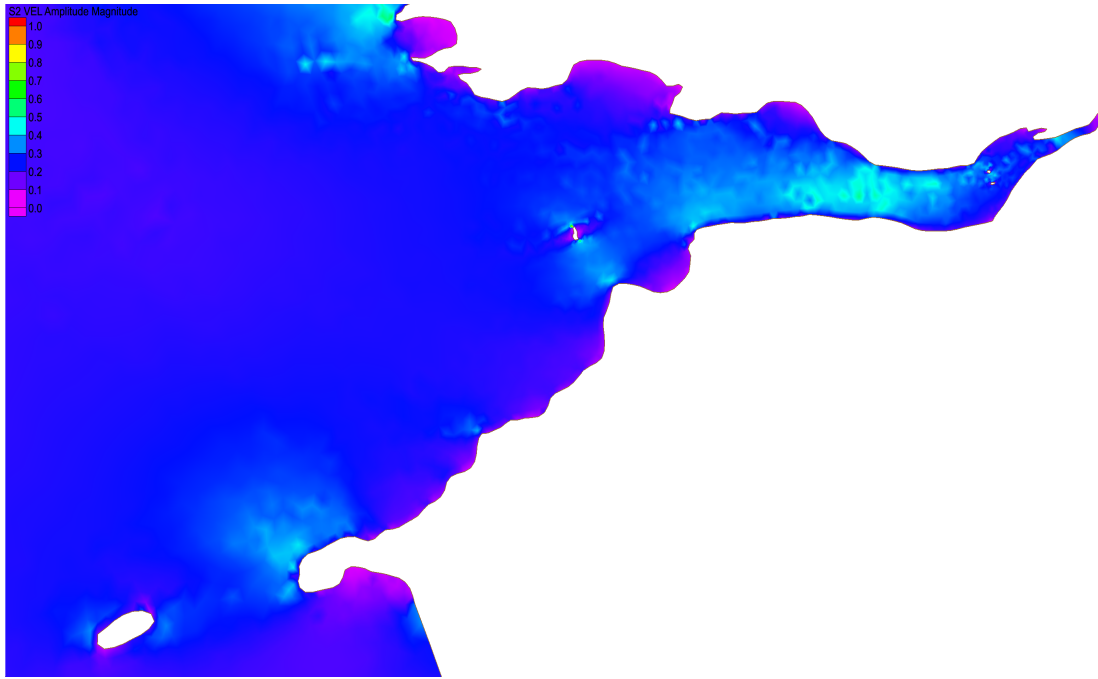


**Figure 16 S<sub>2</sub> tidal current amplitude in the Bristol Channel region (m/s)  
predicted by DG-ADCIRC.**

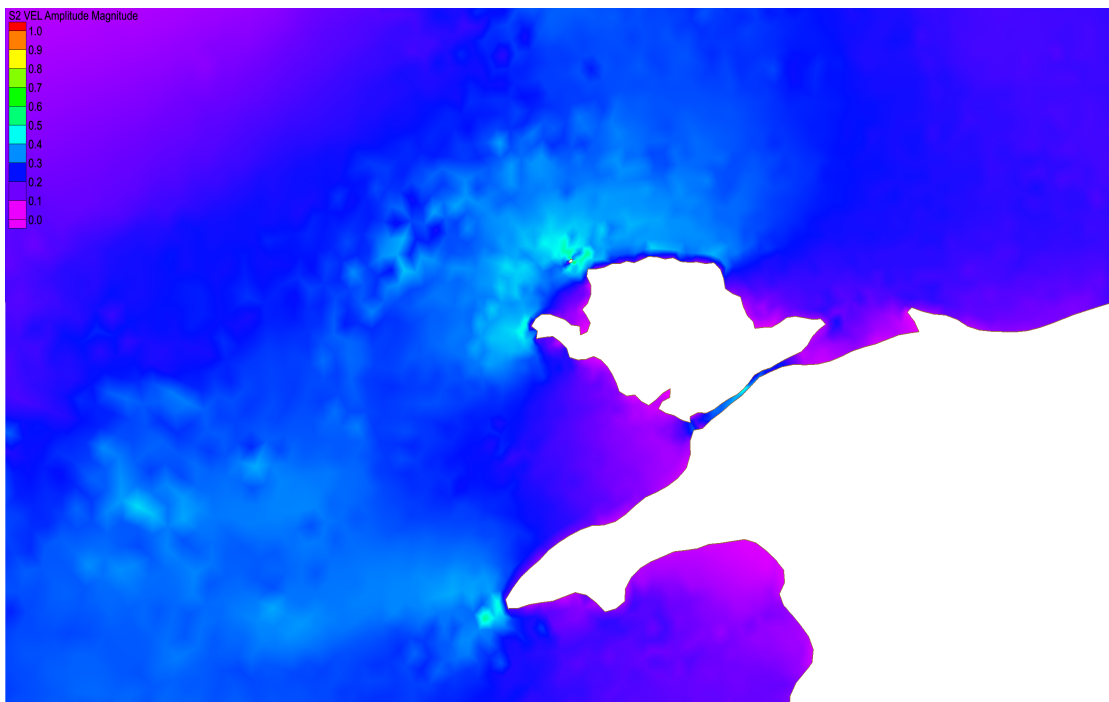


**Figure 17 S<sub>2</sub> tidal current amplitude in the Anglesey region (m/s)  
predicted by DG-ADCIRC.**



### 3.2 The Bristol Channel

This section considers the surface elevations and current velocities predicted for the Bristol Channel. The water elevation comparisons are undertaken against harmonically analysed Total Tide data (Admiralty, 2012). The current velocity comparisons are against Total Tide and BODC data at different locations. Harmonic analysis of observed surface elevation data (obtained from Total Tide software) is used to extract the total contribution of the  $M_2$  and  $S_2$  tides in the regions of interest.

#### *Water Levels*

Figure 18 and Figure 19 show both water surface elevations (relative to mean sea level) for typical flood and ebb tides. Current velocity vectors are superimposed. The figures indicate that the predicted maximum tidal range within this basin is approximately 10.0 m, which is in accordance with observations.

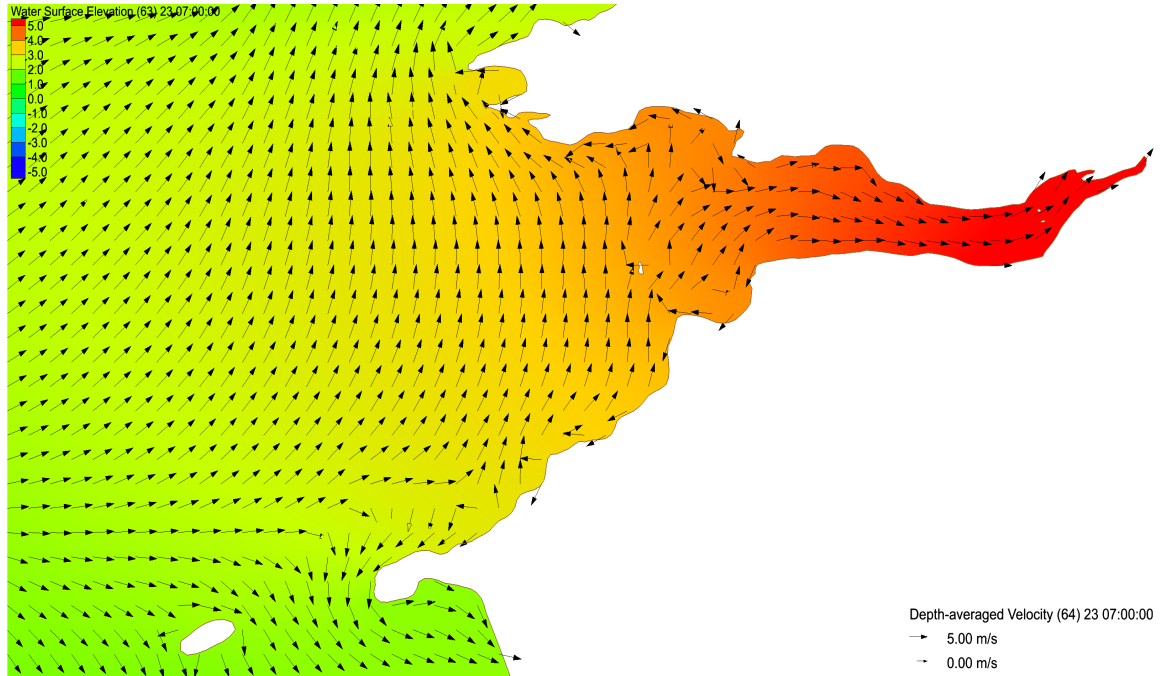


**Figure 18 Water surface elevations (m) and current vectors during a flood tide occurring in the Bristol Channel predicted by DG-ADCIRC.**

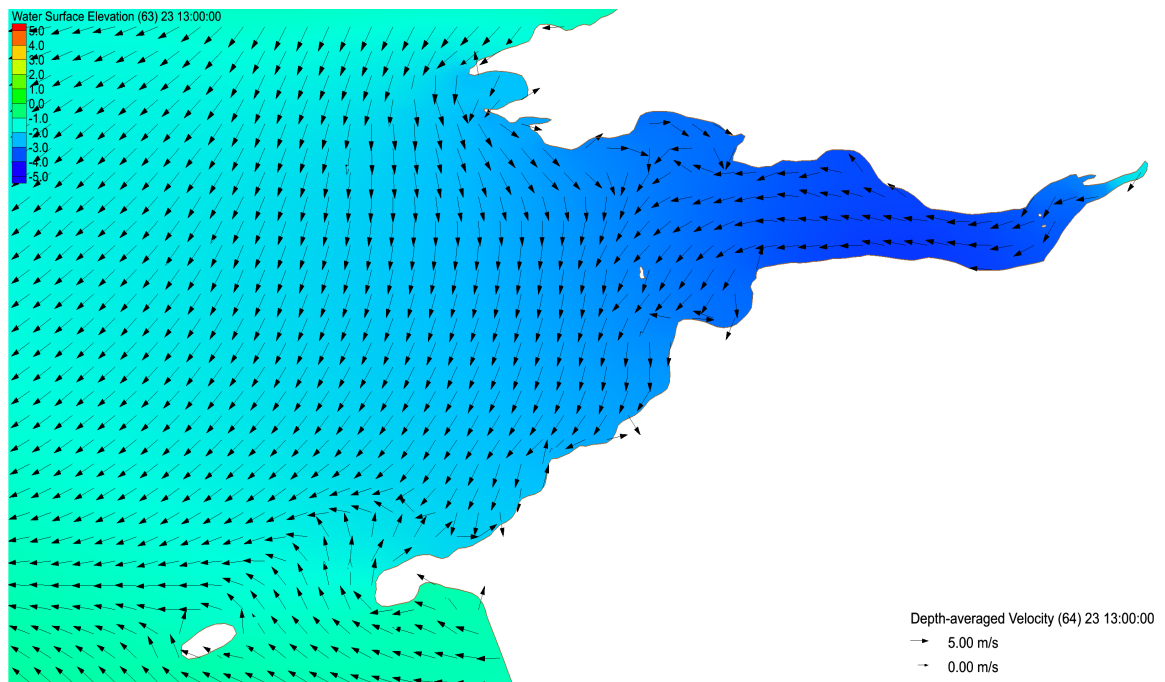


**Figure 19 Water surface elevations (m) and current vectors during an ebb tide occurring in the Bristol Channel predicted by DG-ADCIRC.**

Model predictions of the tidal amplitude are compared against readings from the Admiralty Total Tide at several stations. Figure 20 indicates primary ports (denoted by blue dots), where water levels are estimated by harmonic analysis of *in situ* measurements. Secondary ports (denoted by yellow dots) are locations where the estimated water levels are based on observations from other stations, and may thus be unreliable for validation purposes. For the present validation study, we choose stations at Avonmouth, Barry, Flat Holm, and Ilfracombe for comparison purposes. The simulation period commences on 1<sup>st</sup> January 2012 and runs for a period of 29 days, with a spin up period of one day. Tidal waves are ramped in gradually at the open boundary during the spin-up period in order to reduce the effects of initial transients. For this reason, the characteristics (amplitudes and phases) of the modelled long waves during this period are not representative when compared to the actual characteristics, and so predictions during spin-up period are omitted from the data analysis. Consequently, the prediction results used for comparison purposes start 24 hours after the initial start time. The comparison is presented for 7 days, which starts at 00:00 on 02 January 2012. Figure 21, Figure 22, Figure 23 and, Figure 24 present

comparisons between model predictions and processed measurement of surface elevation at different observation stations.

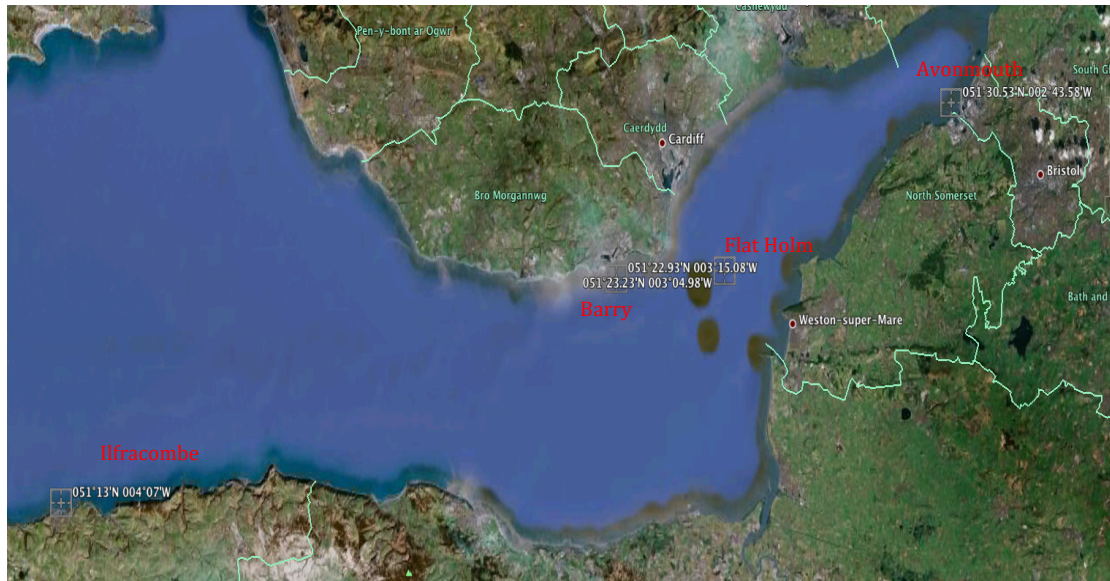


**Figure 20 Locations<sup>2</sup> of the data stations used from the Admiralty Total Tide software for the Bristol Channel (Google Earth)**

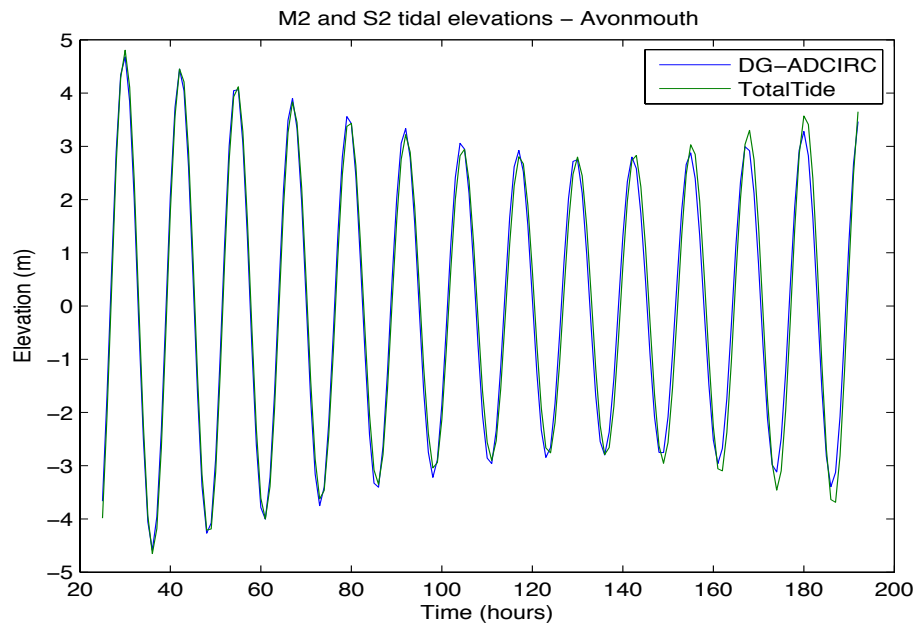


**Figure 21 Predicted (DG-ADCIRC) and analysed (TotalTide) surface elevation levels at Avonmouth, 51°30'N 2°44'W**

---

<sup>2</sup> Previous figure from the Admiralty's TotalTide software replaced with Google Earth satellite image due to improved legibility.

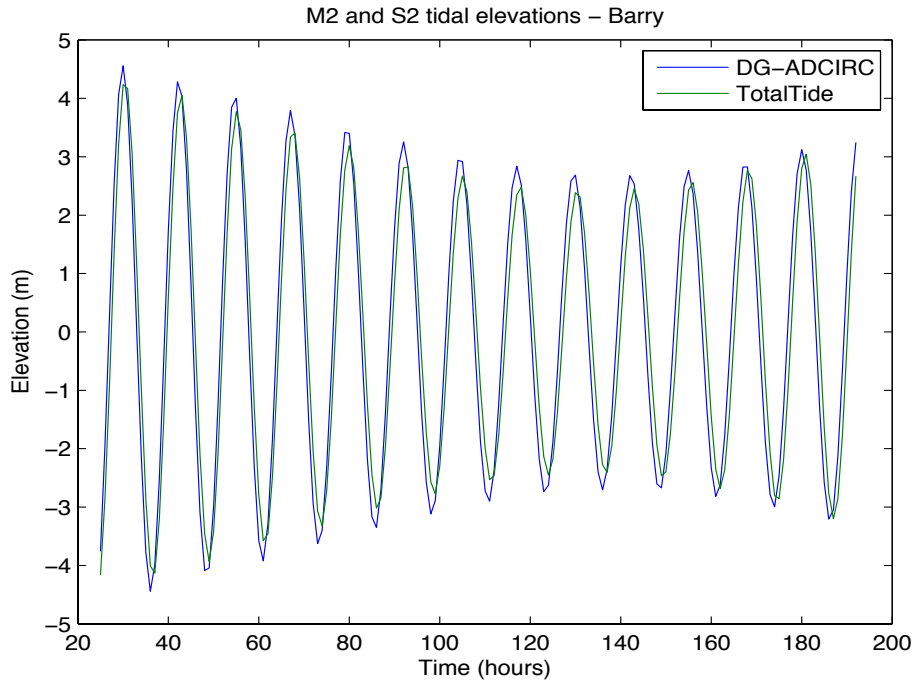


**Figure 22 Predicted (DG-ADCIRC) and analysed (TotalTide) surface elevation levels at Barry, 51°23'N 3°16'W**

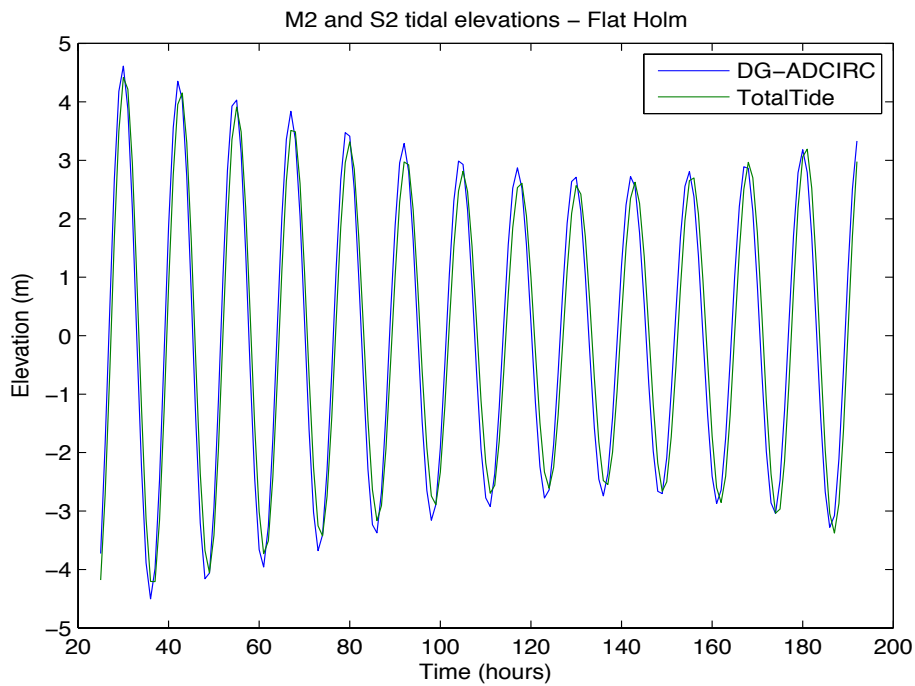


**Figure 23 Predicted (DG-ADCIRC) and analysed (TotalTide) surface elevation levels at Flat Holm, 51°23'N 3°07'W**

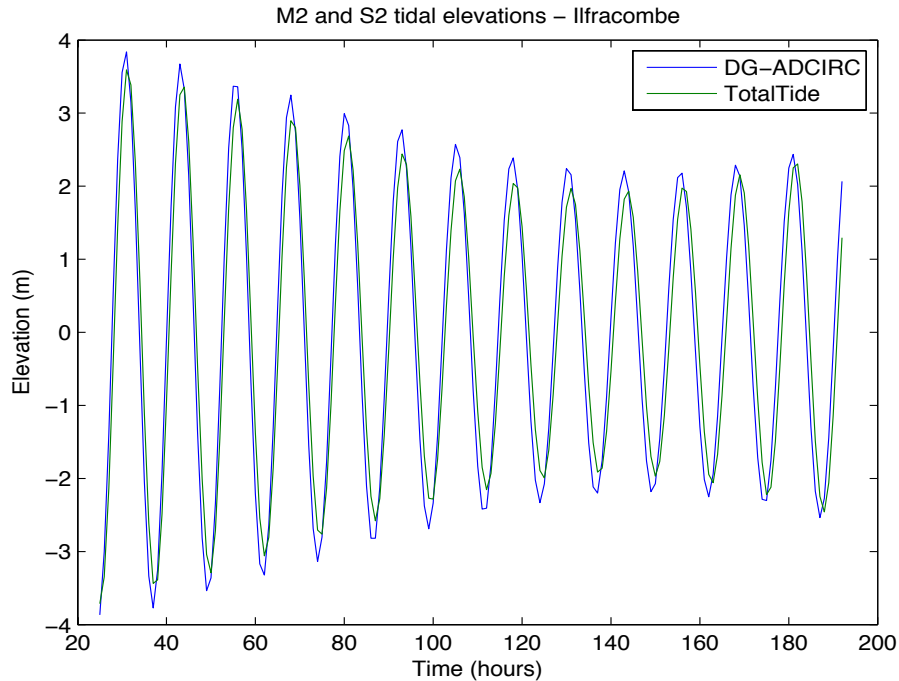


**Figure 24 Predicted (DG-ADCIRC) and analysed (TotalTide) surface elevation levels at Ilfracombe, 51°13'N 4°07'W**

The comparison between the model predictions and the “analysed” data is in excellent agreement with respect to phase. At all stations except Avonmouth, DG-ADCIRC appears slightly to over-predict the amplitude. [It should be noted that we cannot be certain whether the numerical model gives an over-prediction or the interpolations of the field measurements give an underestimate.] A quantitative comparison can be found by harmonic analysis of the results. Table 4 lists observed data, DG-ADCIRC predictions, and alternative results obtained by Davies and Jones (1992) from two-dimensional analysis of the  $M_2$  tidal component. Table 5 gives a similar comparison for  $S_2$  tidal component. The results show that the two-dimensional models under-predict the observed amplitudes and over estimate the phases. When the two-dimensional models are compared, it is evident that DG-ADCIRC model gives better results than the model presented by Davies and Jones (1992). The observed difference in amplitudes is due to the fact that the DG-ADCIRC model uses an unstructured finite element mesh, which is more suitable to represent complex coastlines, with a higher resolution in the Bristol Channel region.

Stations	Observed (TotalTide)		DG-ADCIRC		Davies&Jones (1992) Predictions	
	$H_n(cm)$	$\varphi_n(^{\circ})$	$H_n(cm)$	$\varphi_n(^{\circ})$	$H_n(cm)$	$\varphi_n(^{\circ})$
Avonmouth	432	199	411	206	294	254
Barry	379	184	396	202	333	205
Flat Holm	396	188	402	204	N/A	N/A
Ilfracombe	307	161	325	178	N/A	N/A

**Table 4 Predicted and observed values of  $M_2$  amplitude  $H_n(cm)$  and  $\varphi_n(^{\circ})$**

Stations	Observed (TotalTide)		DG-ADCIRC		Davies&Jones (1992) Predictions	
	$H_n(cm)$	$\varphi_n(^{\circ})$	$H_n(cm)$	$\varphi_n(^{\circ})$	$H_n(cm)$	$\varphi_n(^{\circ})$
Avonmouth	152	274	131	272	86	310
Barry	137	254	125	266	106	255
Flat Holm	137	259	128	268	N/A	N/A
Ilfracombe	112	223	105	234	N/A	N/A

**Table 5 Predicted and observed values of  $S_2$  amplitude  $H_n(cm)$  and  $\varphi_n(^{\circ})$**

### ***Current Velocities***

WG3 WP6 D4A discusses the importance of tidal model validation against current velocity data. Here, we briefly summarise this discussion. The analysis

of currents is different in certain key aspects to the analysis of water surface elevations. One main difference is that the water level observations are a scalar time series, where only the height of the water is recorded, whereas the current observations are a vector time series of current speed and the direction. The reliability of the recorded current data is also affected by elevation of the velocity gauge above the seabed. Data acquired near the seabed are highly sensitive to the exact nature of the local boundary layer, which in turn means that the extrapolation of such data to depth-averaged values is not robust. Current amplitude comparisons are possible using measurements recorded closer to the top of the water column (WG3 WP6 D4A). In the present report, the field current data are plotted using the 1/7<sup>th</sup> power law profile to approximate the mean velocities in a depth-averaged model. The current velocity comparisons are undertaken against,

- a. The Admiralty's Total Tide software current predictions and,
- b. BODC observed field data.

### ***Admiralty Data***

Figure 25 shows the locations for the current readings, taken from the Total Tide software.

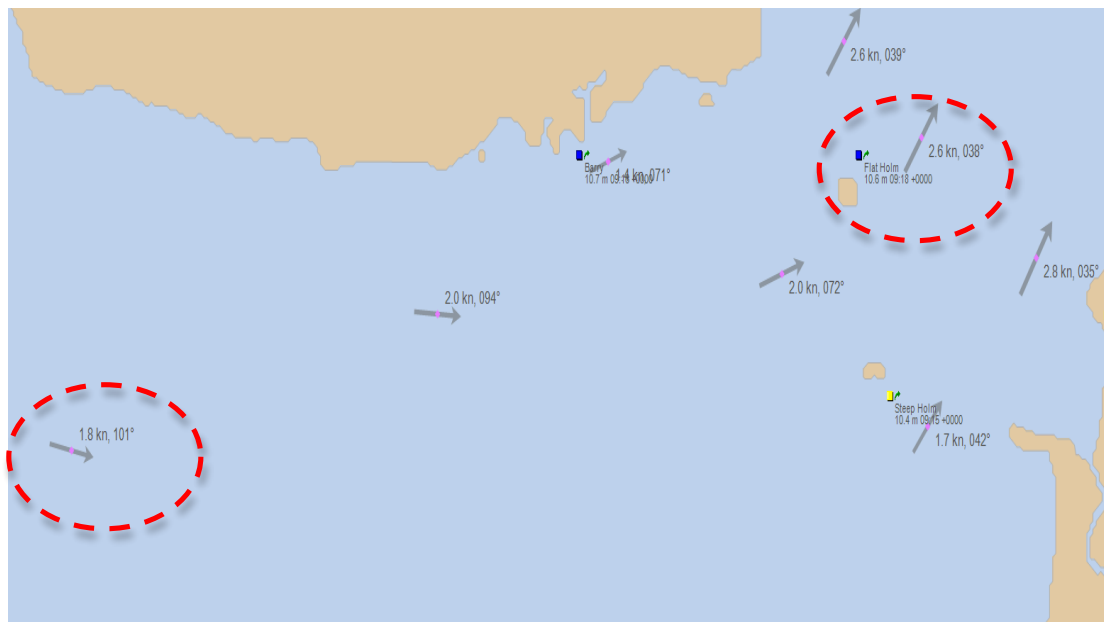


**Figure 25 Current reading stations from Total Tide software for the Bristol Channel region**

The measurements obtained from TotalTide are assumed<sup>3</sup> to be surface velocity measurements, as the software is designed for shipping purposes. Using the 1/7<sup>th</sup> power law, the depth-averaged velocity is calculated using

$$\bar{U}_{mean} = U_{surface} \int_0^h \left( \frac{z}{h} \right)^{1/7} \frac{dz}{h} = \frac{7}{8} U_{surface} \quad 3.2$$

in which  $U_{surface}$  is the surface velocity,  $z$  is distance vertically above the seabed, and  $h$  is the local water depth. Figure 26 and Figure 27 provide plots of predicted and observed hourly currents, starting from 2<sup>nd</sup> January 2012 for a period of 11.5 days.

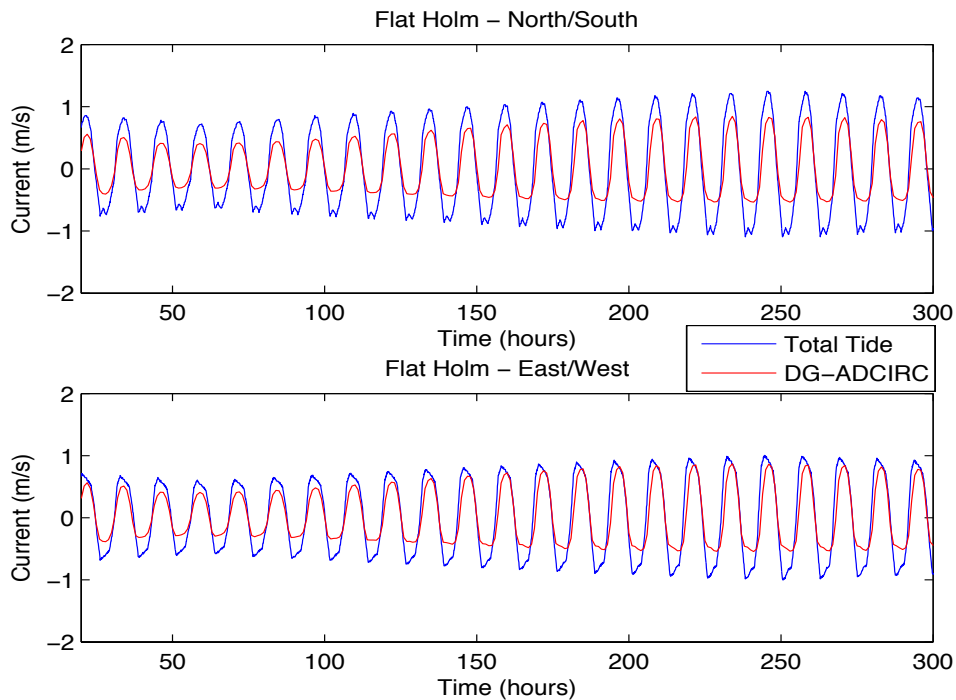


**Figure 26 Predicted and analysed currents at Flat Holm Station, 51°23.23'N 3°04.98'W**

---

<sup>3</sup> There is no information available for the source of measurements undertaken in Total Tide.



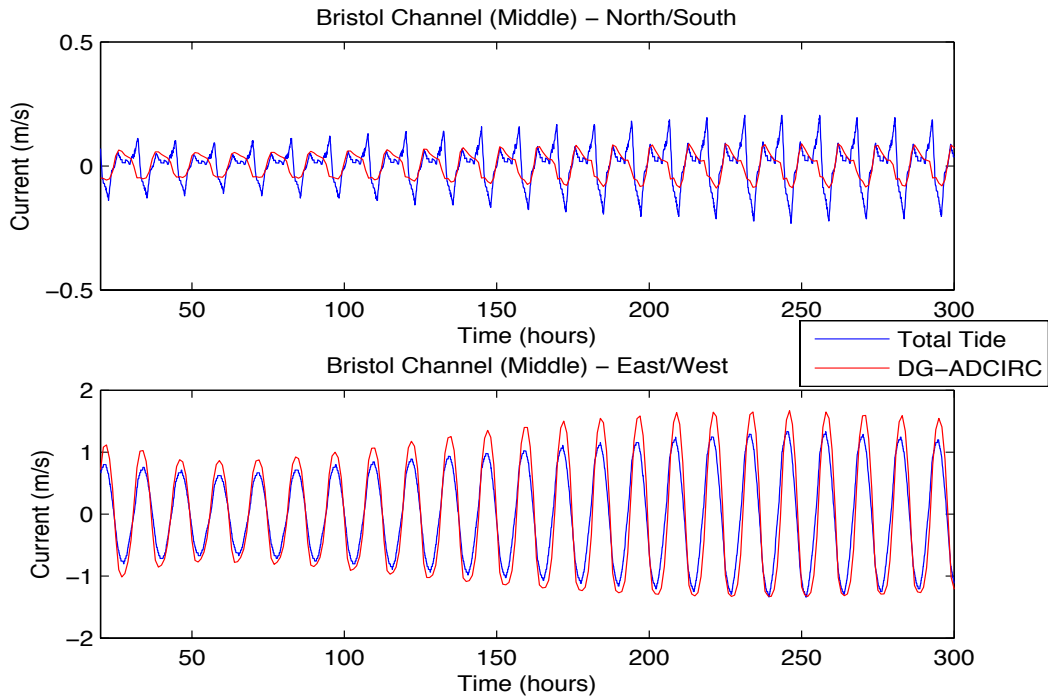


**Figure 27 Predicted and analysed currents at in the middle of the Bristol Channel,  
51°19.33'N 3°32.38'W**

The results show good agreement in terms of phase at both stations. However, the current velocity components are under-predicted at the Flat Holm station in both north/south and east/west directions. At the middle of the Bristol Channel, the north/south current component is under-predicted whereas the east/west current component is over-predicted. A possible explanation for the observed discrepancy between the model predictions and the observed data could be the lack of wetting and drying treatment in the model. A planned action for WG3 WP6 D6 is to include wetting and drying in the model to represent the hydrodynamic response of the region more accurately. Table 6 gives a harmonic analysis comparison between the observed and predicted major semi-diurnal tidal components. The two-dimensional depth averaged hydrodynamic model (DG-ADCIRC) underestimates the current velocity amplitudes in the Flat Holm station. A possible reason for this discrepancy is that the depth-averaged models are not capable of capturing the large eddy formations around the islands. Relatively poor agreement between the model predictions and the observations is expected, where the observation data are gathered in the vicinity of islands of

which eddies are shed. The second observation station used for the current validation is located in the middle of the Bristol Channel (51°19.33'N 3°32.38'W). In this observation station, the predicted and observed currents are in a very good agreement, as shown in Table 6.

Stations	Observed – Total Tide Amplitude of Current Component (m/s)		Predicted DG-ADCIRC Model Amplitude of Current Component (m/s)	
	M <sub>2</sub>	S <sub>2</sub>	M <sub>2</sub>	S <sub>2</sub>
Flat Holm	1.50	0.46	0.77	0.26
Middle of Bristol Channel	1.16	0.38	1.04	0.34

**Table 6 Comparison between observed and predicted tidal current harmonic amplitudes**

### ***Direct Field Measurements - BODC***

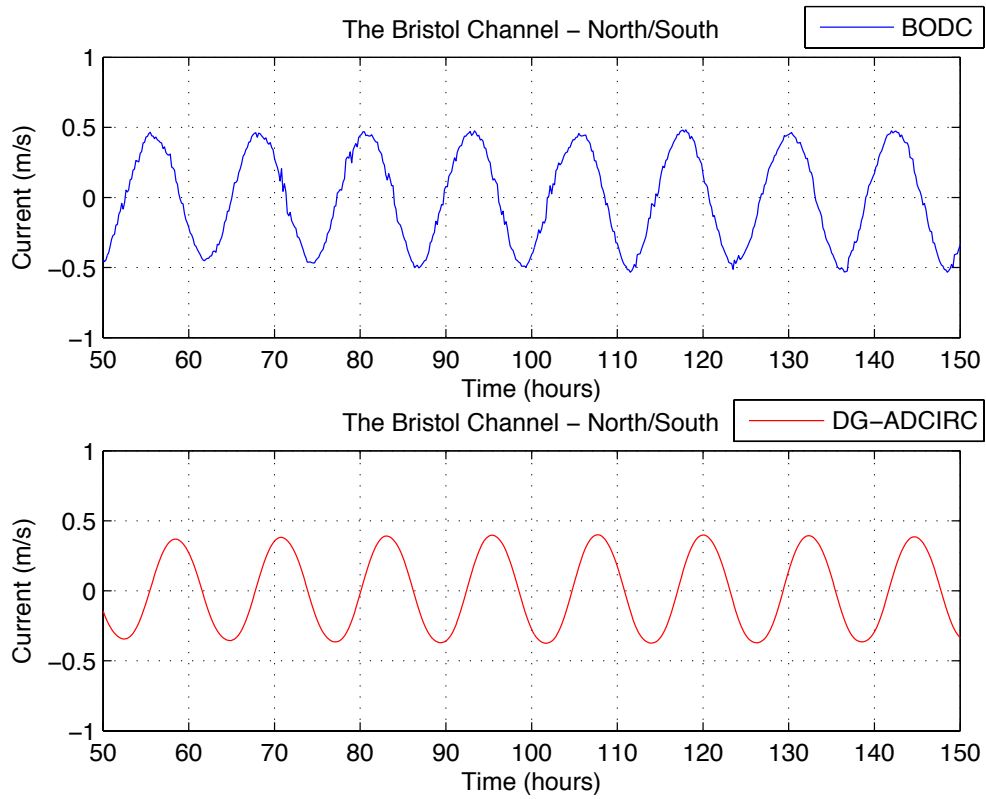
As set out in WG3 WP6 D3, field measurements are available from the British Oceanographic Data Centre (BODC) for a number of sites around the UK. Unfortunately, the recordings of the available current stations are taken very close to the seabed making it impossible to robustly extrapolate to obtain a depth-averaged velocity. There are a number of observation stations, where the data recording is done closer to the water surface, but the duration of the recordings are not generally long enough for a reasonable comparison. Figure 28 shows the selected observation station for comparison. The current measurements are recorded for 10 min intervals, which start on 6<sup>th</sup> June 1975 for 13-days. The water depth in the vicinity of the station is given to be 59.0 m and the current meter had been placed at 23.0 m from the seabed.



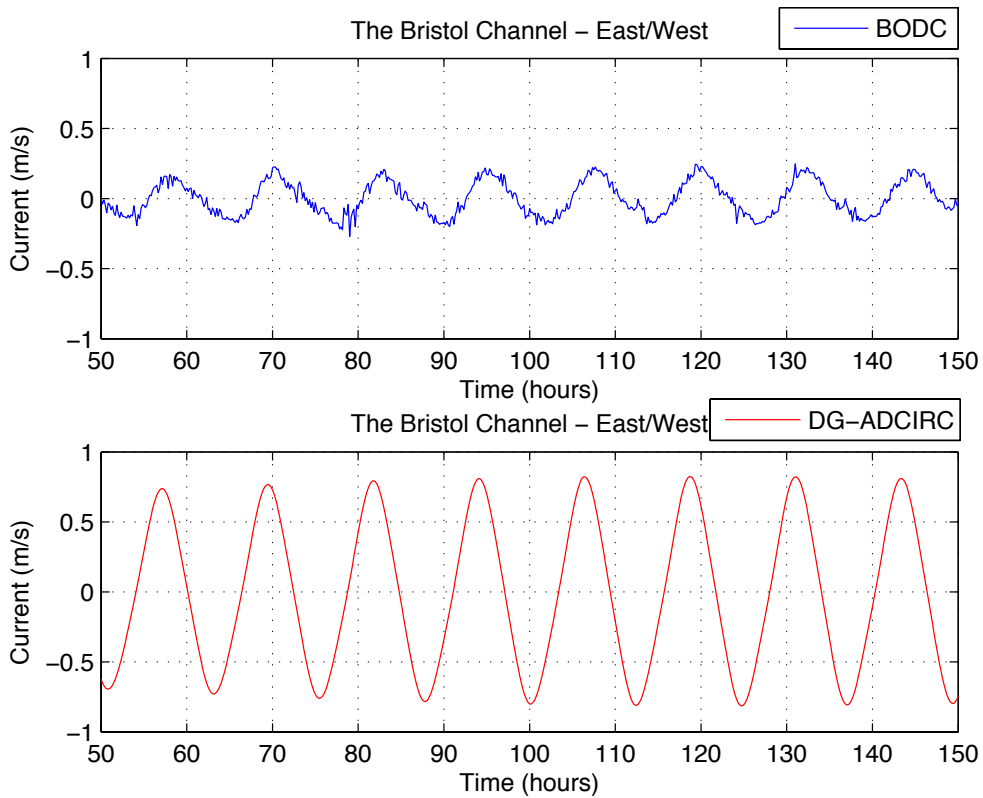
**Figure 28 BODC observation station chosen for the Bristol Channel region,  
51°19.8'N 3°04.51.6'W (Google Earth)**

Figure 29, Figure 30 and, Figure 31 show the current comparisons between the observations and the model for 100 hours. Harmonic analysis (Pawlowicz, *et al.*, 2002) has been undertaken on the modelled current results to predict the tides occurring on the time period of the observations. There is a minor phase difference between the modelled and observed data in both east-west and north-south directions. In terms of current components, a good agreement is seen in north-south direction, whereas the model is over-predicting the currents occurring in east-west direction. As the measured data were sampled closer to the seabed, small discrepancies might occur in terms of the magnitude of the currents. Predicted and observed current directions are shown in Figure 32. The convention used in the plot is that zero degrees is in the eastward direction, and the angle is positive in the anti-clockwise direction. Figure 32 suggests that the general pattern of the current directions is well captured by the model, although there is a 3 hr phase difference between the predicted and observed direction. The reasoning behind this discrepancy is still under investigation. One possible explanation for this difference is thought to be due to the altered coastline datum. As wetting and drying treatment is not included in the analysis, the coastline in the region is interpolated with a mean sea level of 6.0 m. Thus the

phase of the reflected waves from the shoreline is prone to be in error with the incoming wave phase.



**Figure 29 Predicted and observed currents in N/S direction at 51°19.8'N 3°04.51.6'W**



**Figure 30 Predicted and observed currents in E/W direction at 51°19.8'N 3°04.51.6'W**

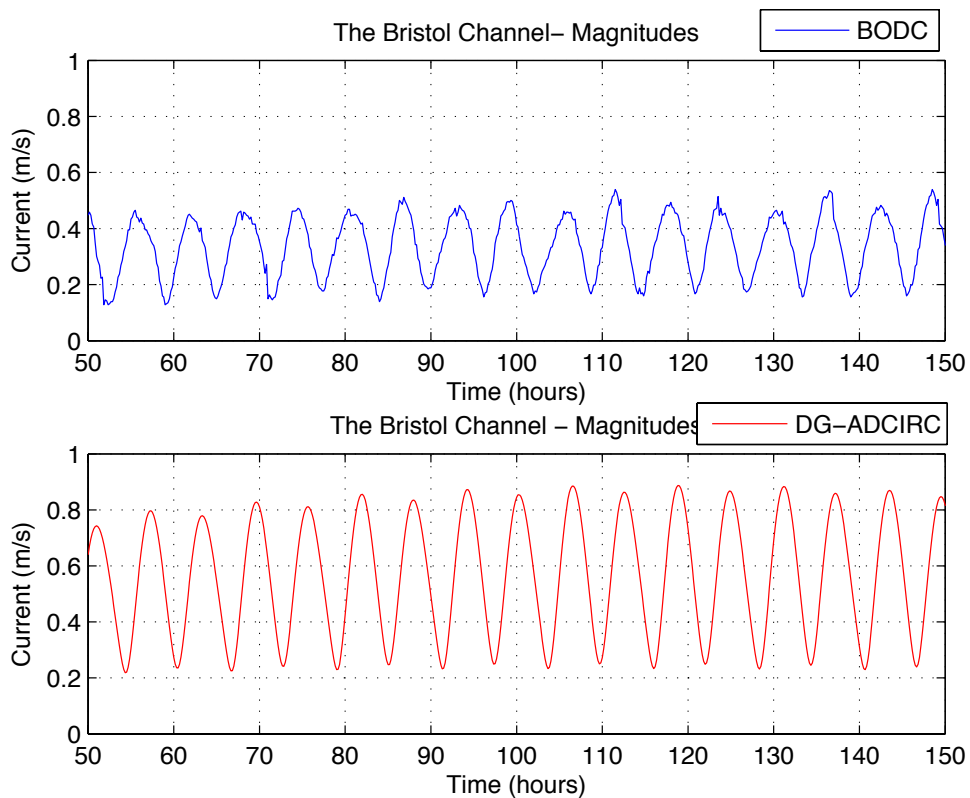


**Figure 31 Predicted and observed current magnitudes at 51°19.8'N 3°04.51.6'W**

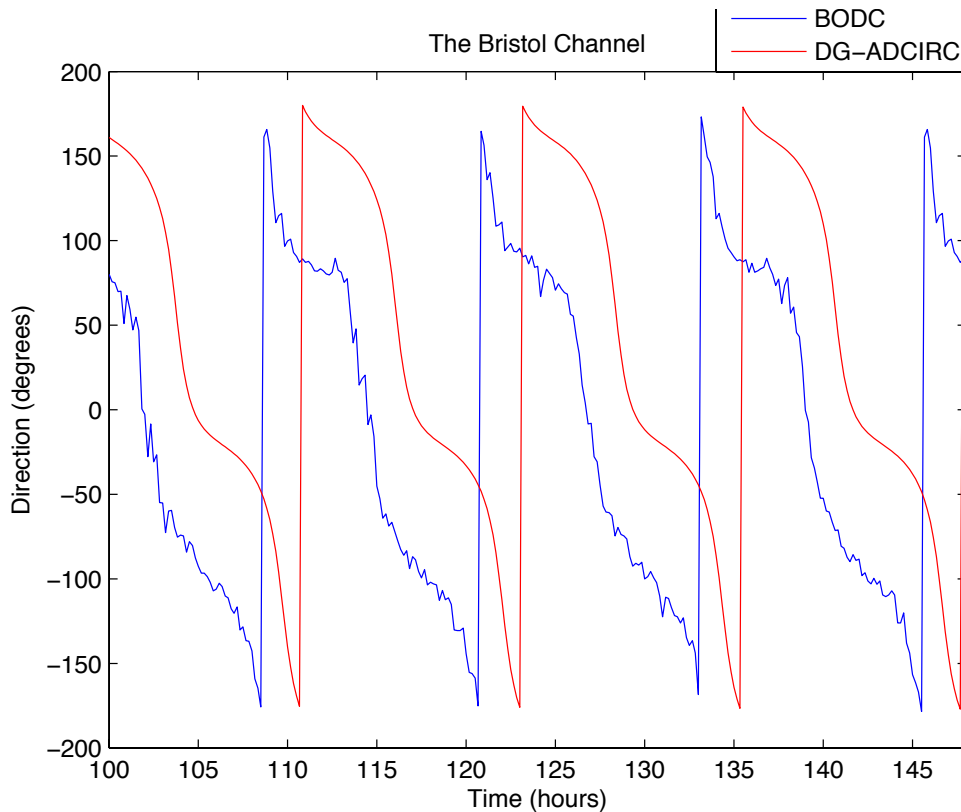


**Figure 32 Predicted and observed current directions at 51°19.8'N 3°04.51.6'W**

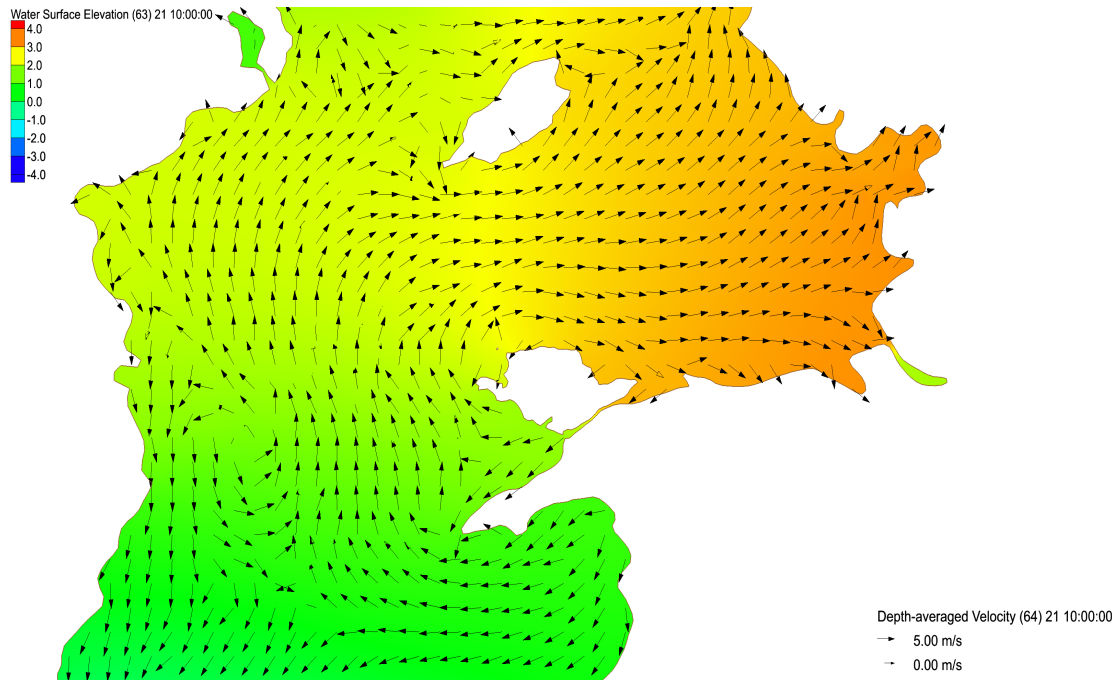
### 3.3 Anglesey

This section investigates the model validation for Anglesey, and follows the same format as Section 3.2. In the first subsection, model predictions are presented of surface elevation and comparisons against field data. The second subsection considers the current velocities.

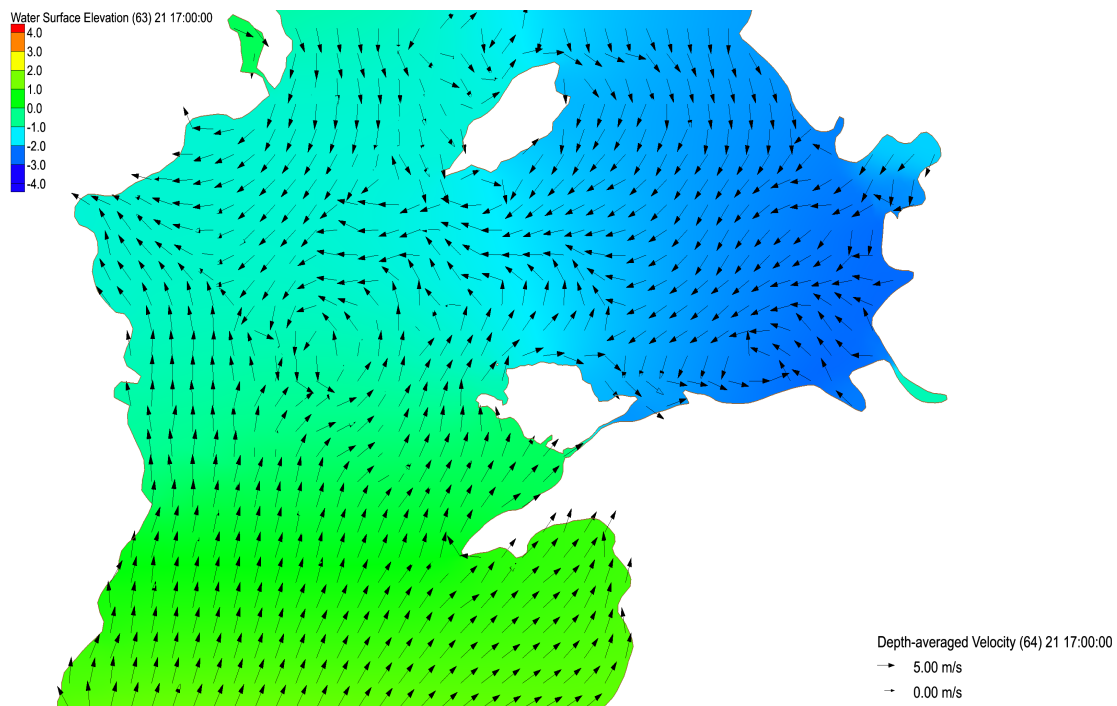
#### *Water Levels*

Figure 33 and Figure 34 show the water surface elevations (relative to mean sea level) for typical flood and ebb tides respectively. The current velocity vector fields are superimposed. It is evident that the energy of the incoming wave from the south is dissipated when propagating to the north due to the formation of the amphidromic system on the Irish coast. The Coriolis force from the Earth's rotation affects the propagation of the tide, leading to a difference in tidal range

between the Irish coasts and the coasts of Wales and England (Howarth 1984). The tidal range difference can be seen in the figures below.



**Figure 33 Water surface elevation distribution and current field during a flood tide in the vicinity of Anglesey, predicted by DG-ADCIRC. Contours = water elevations (m); vectors = maximum current (m/s)**



**Figure 34 Water surface elevation distribution and current field during an ebb tide in the vicinity of Anglesey, predicted by DG-ADCIRC. Contours = water elevations (m); vectors = maximum current (m/s)**

For Anglesey, the model predictions are compared against amplitude readings from Admiralty Total Tide at Holyhead, Cemaes Bay and Amlwch. The coverage of the Anglesey region is given in Figure 35.

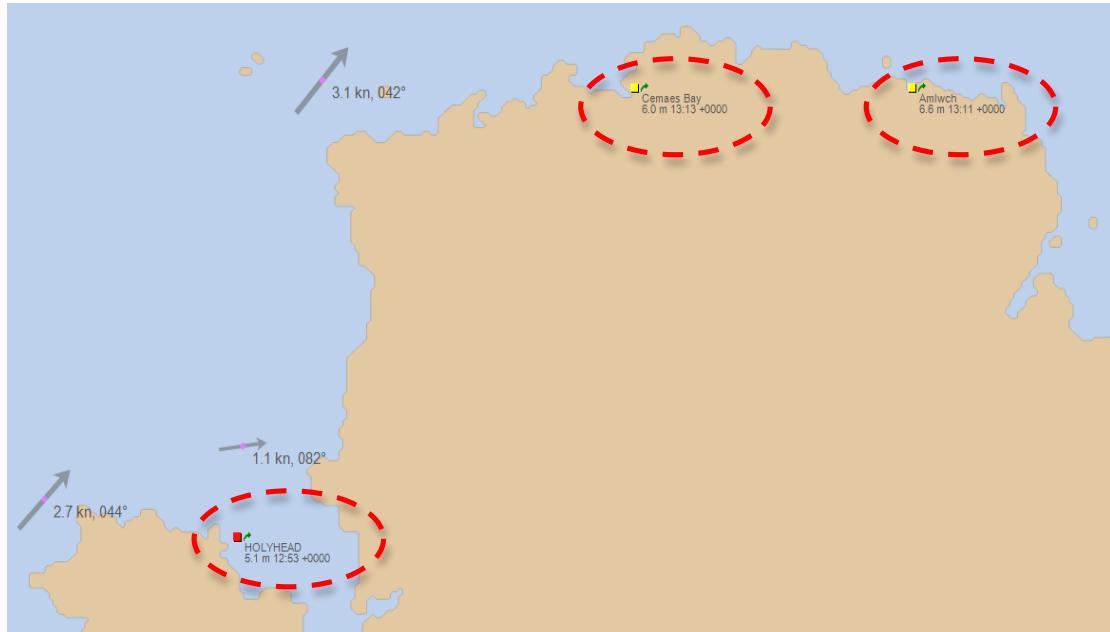
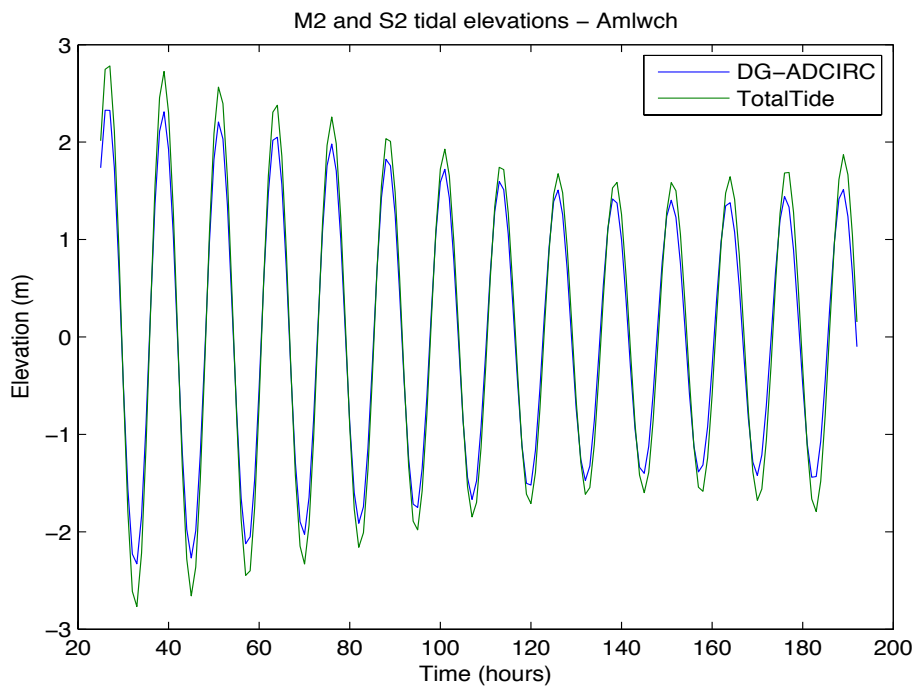


**Figure 35 Data available from the Admiralty Total Tide software for Anglesey. Red dashed circles indicate ports used for validation. Arrows indicate tidal stream direction.**

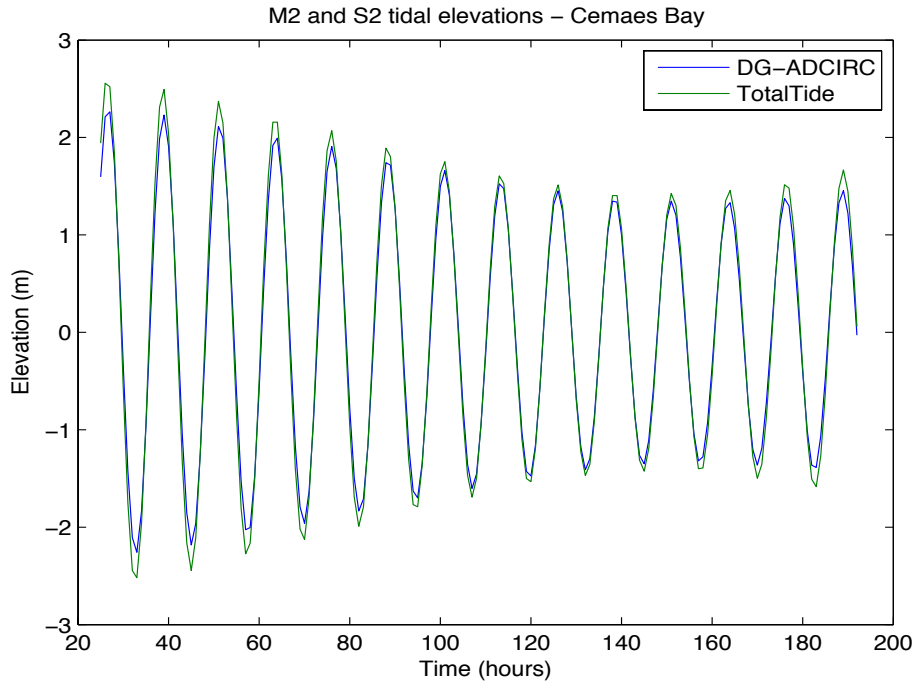
Figure 36, Figure 37 and, Figure 38 present comparisons between the model predictions and the processed measurements of sea surface elevation time histories at the selected stations. The predictions and observations are in good agreement with respect to phase. Tidal amplitude is under-predicted, which may be due to the use of a relatively high uniform bed friction coefficient throughout the computational domain. In practice, bed friction will vary continuously across the domain. However, it is impractical to reproduce the change in bed friction spatially in a numerical model correctly. As discussed in WG3 WP6 D4A, the appropriate value for bed friction may be anisotropic (varying with direction) and also may not be constant with flow velocity. Soulsby (1998) gives a range of suggested values for different sea and bed conditions, which may be applied spatially in the numerical model. However, the accuracy of the model is not always guaranteed (Richard Soulsby, personal communication). Table 7 and



Table 8 list the predicted and observed  $M_2$  and  $S_2$  tidal constituents. Table 7 indicates that there is a very good agreement in  $M_2$  phases. The  $M_2$  amplitudes however are underestimated by  $\sim 10\%$ . Considering the  $S_2$  tidal constituent, the phases are slightly under estimated, as well as the amplitudes. This discrepancy in amplitudes is due to the higher bed-friction coefficient used in the overall model. Although, there is a slight difference between the observed and predicted amplitudes and phases, the overall model results show an excellent agreement with the global hydrodynamics of the region.



**Figure 36 Predicted and analysed surface elevation levels at Amlwch, 53°25'N 4°20'W**



**Figure 37 Predicted and analysed surface elevation levels at Cemaes Bay, 53°25'N 4°27'W**

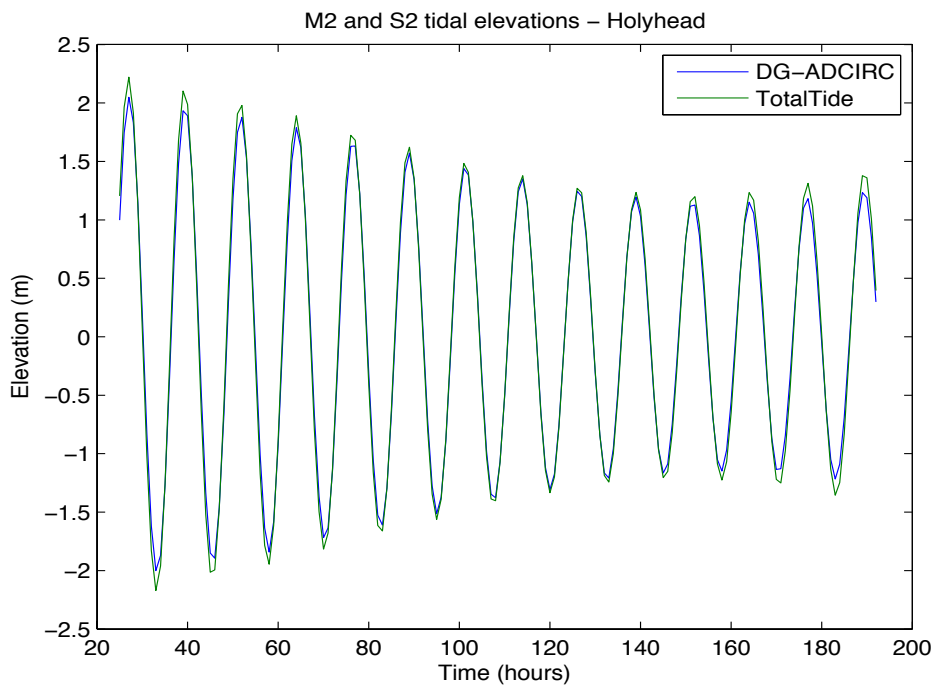


**Figure 38 Predicted and analysed surface elevation levels at Holyhead, 53°19'N 4°37'W**

Stations	Observations Total Tide		DG-ADCIRC Predictions	
	$H_n(cm)$	$\varphi_n(^{\circ})$	$H_n(cm)$	$\varphi_n(^{\circ})$
Amlwch	237	302	198	306
Cemaes Bay	215	305	190	303
Holyhead	182	290	166	289

**Table 7 Predicted and observed values of  $M_2$  amplitude  $H_n(cm)$  and  $\varphi_n(^{\circ})$**

Stations	Observations Total Tide		DG-ADCIRC Predictions	
	$H_n(cm)$	$\varphi_n(^{\circ})$	$H_n(cm)$	$\varphi_n(^{\circ})$
Amlwch	77	357	58	352
Cemaes Bay	72	358	56	349
Holyhead	60	343	51	333

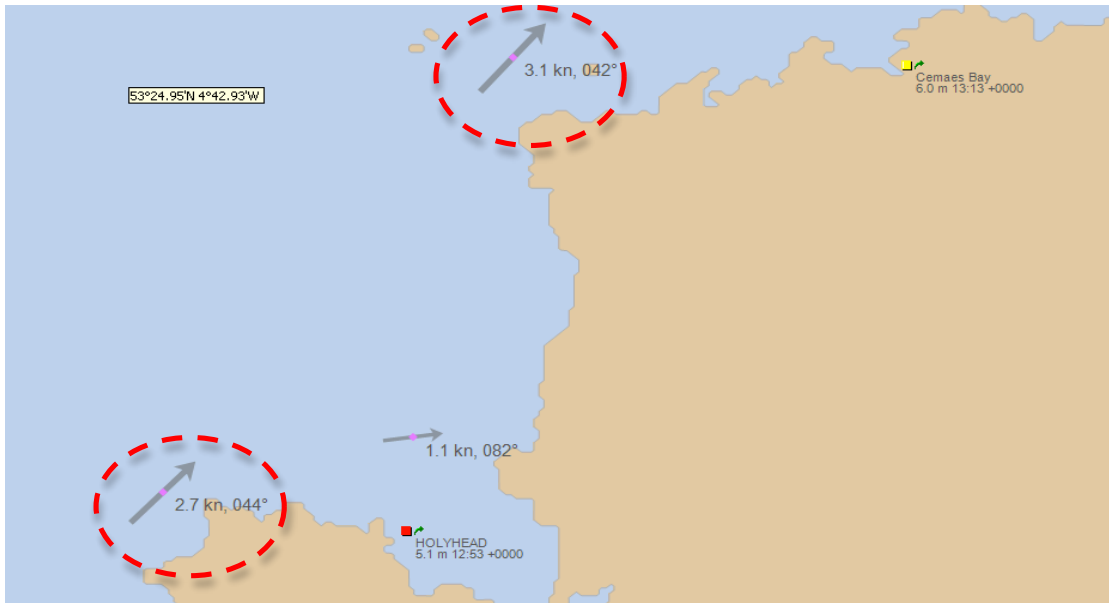
**Table 8 Predicted and observed values of  $S_2$  amplitude  $H_n(cm)$  and  $\varphi_n(^{\circ})$**

### ***Current Velocities***

Model validation against observed current velocities in the Anglesey region is undertaken using two sets of data: interpolation of observed data by the Admiralty's Total Tide software; and observed current data obtained from BODC. We observe that there are in reality, large eddies around the Anglesey coast. Depth-averaged models cannot model these accurately, so good agreement between the field data and the model is not expected (Stansby, 2006).

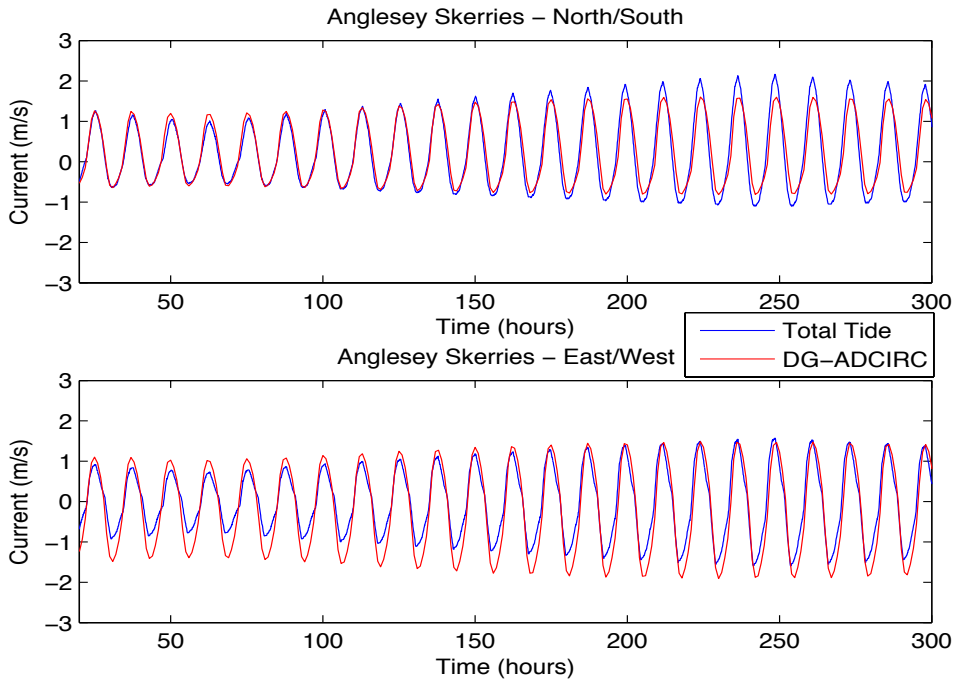
## Admiralty Data

Figure 39 shows the Total Tide current stations.



**Figure 39 Current recording stations in Total Tide software for the Anglesey region (indicated by dashed red circles)**

Figure 40 and Figure 41 show predicted and observed current (hourly) time histories at Anglesey Skerries and Holyhead, starting from 2<sup>nd</sup> January 2012 for a period of 11.5 days.



**Figure 40 Predicted and observed currents at Anglesey Skerries, 53°25.11'N 4°34.87'W**

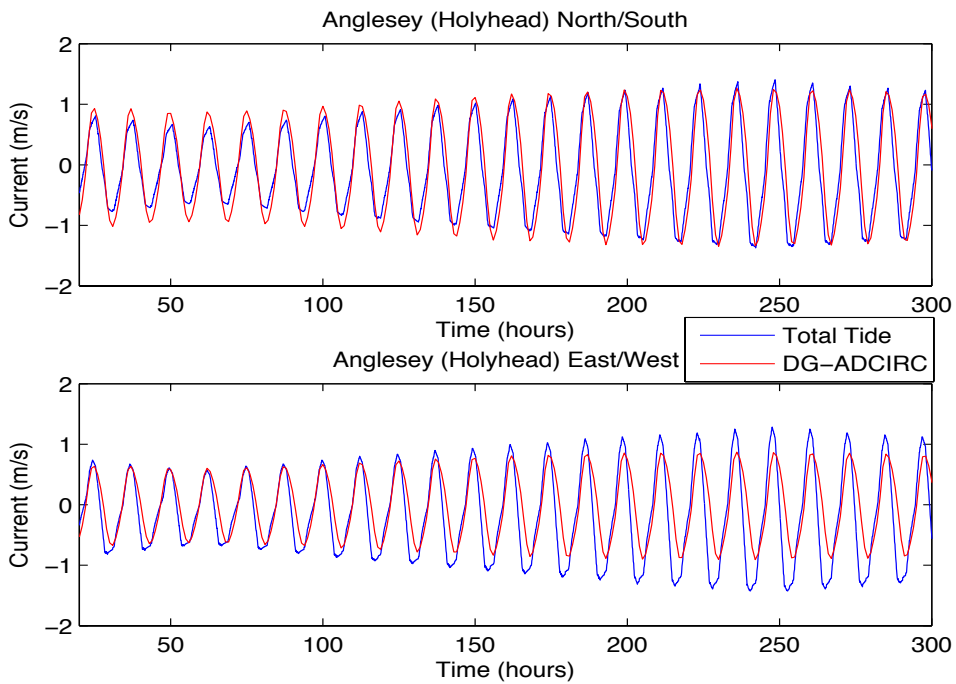


**Figure 41 Predicted and observed currents at Holyhead, 53°19.51'N 4°41.87'W**

The predicted phase is in good agreement with observations at Anglesey Skerries for both north-south and east-west current components. However, the north-south current amplitude is under-predicted and the east-west current

amplitude is over-predicted, indicating that the direction of the current is slightly in error. At Holyhead, there is close agreement between the predicted and observed phase of the north-south current component, but a slight phase shift is evident in the east-west current component. The predicted amplitude of the north-south current component is in acceptable agreement with the observed component. However, the model underestimates the current amplitudes in the east-west direction. Table 9 compares the observed and predicted amplitudes of the major semi-diurnal tidal current components obtained using harmonic analysis. The model underestimates the current amplitudes in the Anglesey Skerries station. The discrepancy in direction may be due to inaccuracy in the representation of eddies in the depth-averaged models. The results obtained from the Holyhead station show a closer agreement with the observations.

Stations	Observed – Total Tide		DG-ADCIRC Model	
	M <sub>2</sub>	S <sub>2</sub>	M <sub>2</sub>	S <sub>2</sub>
Angl. Skerr.	1.92	0.62	1.60	0.40
Holyhead	1.60	0.51	1.67	0.43

**Table 9 Comparison of tidal current harmonic amplitudes (m/s)**

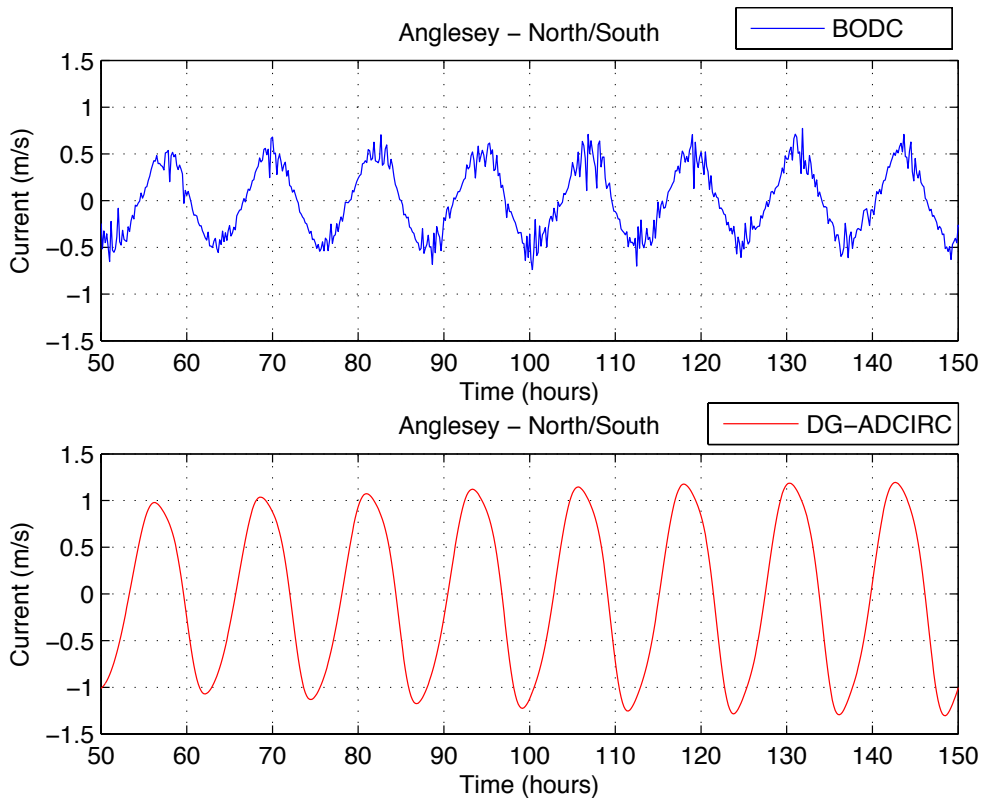
### ***Direct Field Measurements - BODC***

Figure 42 shows the location of the selected observation station in the Anglesey region. The water depth in the vicinity of the station is given to be 44.0 m and the current meter is placed on 31.0 m above the seabed. The current recordings started on 1<sup>st</sup> November 1968 for a period of 16-days.



**Figure 42 BODC observation station chosen for the Anglesey region,  
53°17.5'N 3°04.55.0'W (Google Earth)**

Figure 43 and Figure 44 show the current comparisons between the observations and the model for 100 hours. Harmonic analysis (Pawlowicz, *et al.*, 2002) has been undertaken on the modelled current results to predict the tides occurring on the time period of the observations. There is a minor phase difference between the modelled and observed data in north-south direction. On the other hand, the predicted currents in east-west direction are 180° out of phase. Bearing in mind that the depth-averaged models are not efficiently capturing the large eddy formation, it is expected to have a rather poor agreement in current component comparisons. Figure 45 shows the total current magnitude comparison between the observations and the model. It is seen that overall, there is a slight phase difference between the model predictions and observations. The magnitude of the currents, however, is over-predicted by the model. The direction of the predicted and observed currents is presented in Figure 46. The convention used in the plot is that zero degrees is towards east and, the angle is positive in the anti-clockwise direction. The predicted current directions differ typically by about 50 degrees from the BODC observations, on both the flood tides, indicating that the model has not entirely captured the direction of the tide at this location.



**Figure 43 Predicted and observed current on N/S direction at 53° 17.5'N 3° 04.55.0'W**

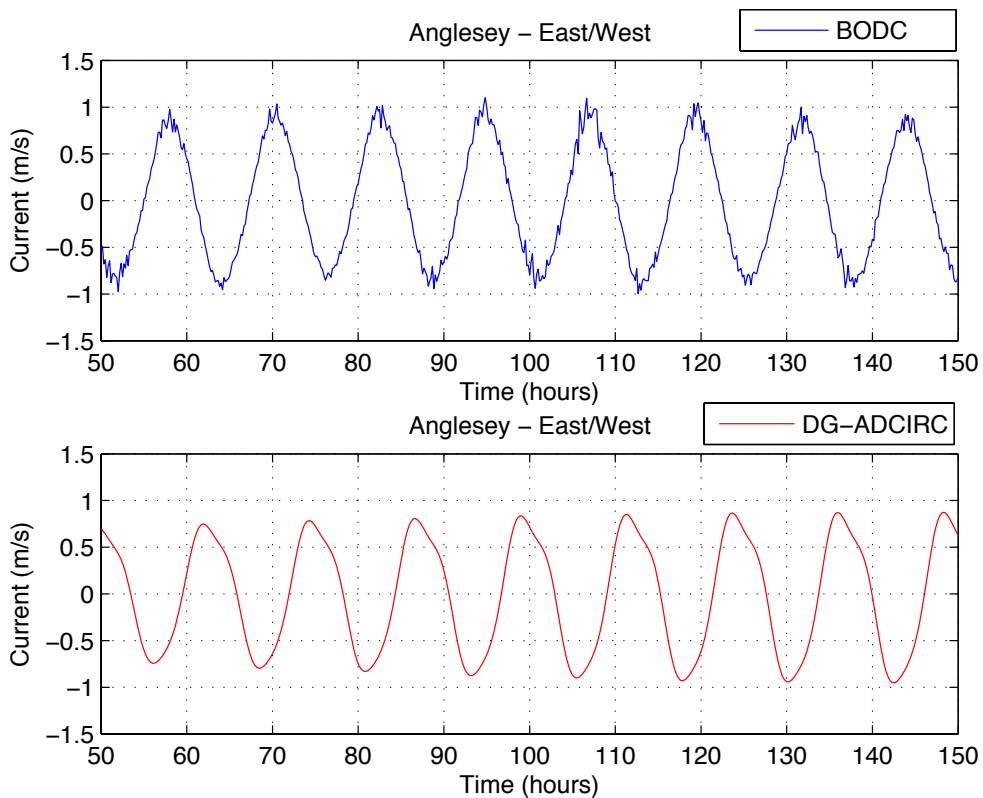


**Figure 44 Predicted and observed current on E/W direction at 53° 17.5'N 3° 04.55.0'W**



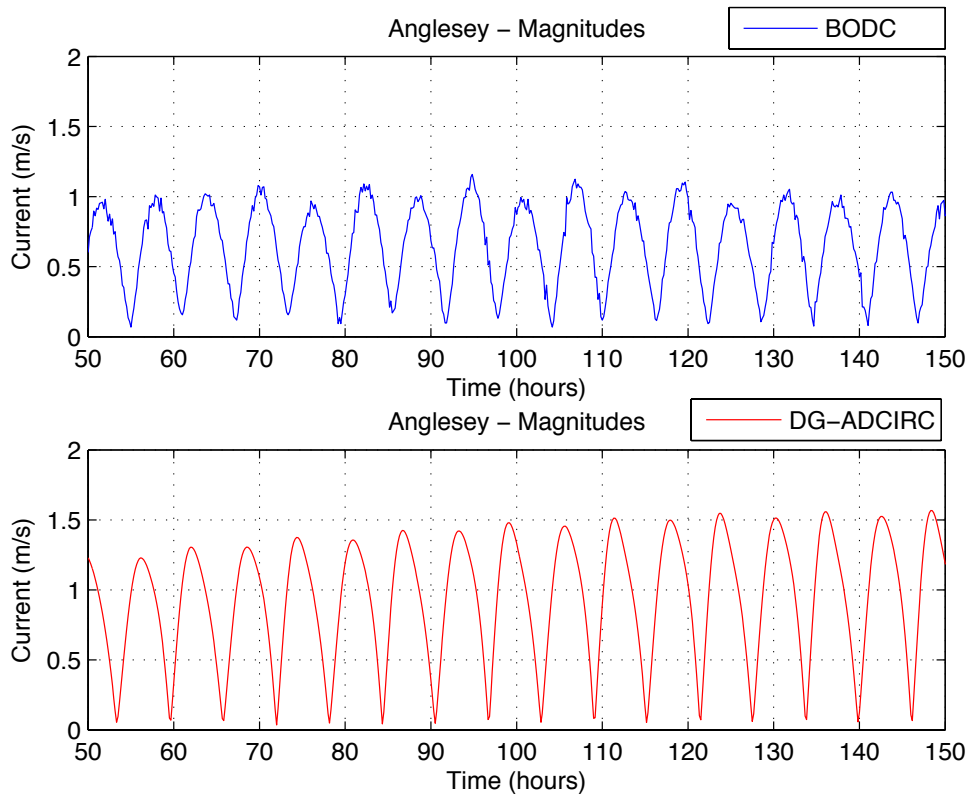


**Figure 45 Predicted and observed current magnitudes at 53°17.5'N 3°04.55.0'W**

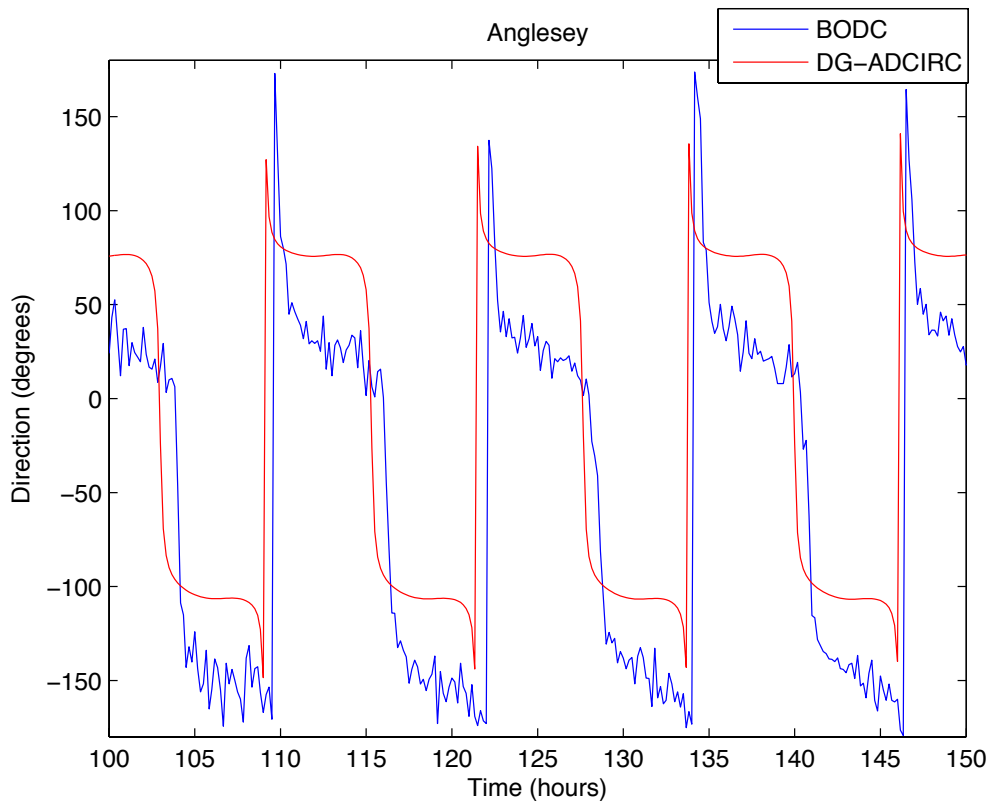


**Figure 46 Predicted and observed current directions at 53°17.5'N 3°04.55.0'W**

## ***Conclusions***

A calibrated model of the  $M_2$  and  $S_2$  tidal flows in the South West coasts of the UK is presented, focusing particularly on the Bristol Channel and Anglesey regions. The model extends outward to the continental shelf, and is forced with appropriate tidal elevations. Comparisons with independent data sources demonstrate that the overall model achieves a very good prediction of the pattern of tidal elevations throughout the region analysed. Detailed comparisons with individual stations demonstrate some minor discrepancies, but again agreement on elevations is good.

Comparisons with current measurements are intrinsically more difficult because of uncertainties attaching to the observations. However, where comparisons have been possible they indicate an agreement that is satisfactory. Differences are apparent in detailed response (e.g. when considering N-S and E-W currents separately), but overall current magnitudes are approximately correct. Bearing in mind the limitations of the depth-averaged models, discussed in WG3 WP6 D2, rather poor representation of currents is expected in regions where large eddies occur.

The shortcomings of the current model are understood. These relate primarily to two aspects:

- a. the use of a single overall bed friction coefficient and,
- b. the omission of wetting and drying from the analysis.

As more detailed models of tidal extraction are developed for the two sites of interest, the opportunity will be taken to refine the bed friction values to achieve closer agreement. Analyses of the Bristol Channel region including wetting and drying will also be made for comparison, which will be presented in WG3 WP6 D6.

## References

- Adcock, T. A. A., Borthwick, A. G. L., and Houlby, G. T., The open boundary problem in modelling tidal energy extraction, EWTEC, Southampton, 2011.
- Admiralty, 2006, *North coast of Scotland pilot*. N.P. 52. Hydrographic office, Taunton.
- Bunya, S., Kubatko, E. J., Westerink, J., J., and Dawson, C., A wetting and drying treatment for the Runge-Kutta discontinuous Galerkin solution to the shallow water equations, *Comput. Methods Appl. Mech. Engg.*, 198, 2009, p:1548-1562.
- Davies, A.M., and Jones, J.E. 1992, A three dimensional model of the M<sub>2</sub>, S<sub>2</sub>, N<sub>2</sub>, K<sub>1</sub> and O<sub>1</sub> tides in the Celtic and Irish Seas, *Prog. Oceanog.* **29**:197-234.
- Doodson, A.T., 1921, The Harmonic Development of the Tide-Generating Potential. *Proceedings of the Royal Society of London, Series A*, **100**: 305-329
- Howarth, M.J. 1984, Currents in the Eastern Irish Sea, *Oceanography and Marine Biology An Annual Review*, **22**:2-47, Aberdeen University Press.
- Kubatko, E., Dawson, C., and Westerink, J.J. 2008, Time step restrictions for Runge-Kutta discontinuous Galerkin methods on triangular grids, *Journal of Computational Physics*, 227: 9697-9710.
- Le Provost, C. 1991, Generation of overtides and compound tides. In *Tidal Hydrodynamics*, ed. B. B. Parker. John Wiley & Son.
- Le Provost, C., Genco, M. L., and Lyard, F. 1995, Modeling and predicting tides over the World Ocean, *Quantitative Skill Assessment for Coastal Ocean Models, Coastal and Estuarine Studies*, **47**: 175-201
- Monahan, D. 2008, Application of the General Bathymetric Chart of the Oceans (GEBCO) Digital Atlas in the delineation of continental shelves under Article 76 *Journal of Ocean Technology*, **3**: 24-29
- Pawlowicz, R., Beardsley, B., Lentz, S. 2002, Classical tidal harmonic analysis including error estimates in MATLAB using T\_TIDE, *Computers & Geosciences*, **28**(8): 929-937

- Pugh, D.T. 1987, *Tides, Surges and Mean Sea-Level*, John Wiley and Sons.
- Robinson, I.S. 1978, The tidal dynamics of the Irish and Celtic Seas, *Geophys. J. R. Astr. Soc.*, **56**: 159-197.
- Soulsby, R., *Dynamics of Marine Sands*. Thomas Telford, 1998.
- Stansby, P. K., Limitations of Depth-Averaged Modelling for Shallow Wakes, *Journal of Hydraulic Engineering*, 132 (7), 2006, p: 737-740.
- Tu, S., and Aliabadi, S. 2005, A Slope Limiting Procedure in Discontinuous Galerkin Finite Element Method for Gasdynamics Application, *International Journal of Numerical Analysis and Modeling*, 2(2): 163-178.

## ***Appendix 1: Bathymetry data***

The digitised bathymetry was derived from raw data supplied in “ascii” format by Seazone (<http://www.seazone.com>). A MATLAB script for converting these data to  $x, y, z$  format ready for importing to the meshing software is included with the present deliverable. The areas needed for this simulation are

**Survey gridded bathymetry:** NW55100035.asc, NW55100040.asc,  
NW55100045.asc, NW55100050.asc, NW55150045.asc, NW55150050.asc,  
NW55300045.asc, NW55300050.asc

**Chartered gridded bathymetry:** NW24800060.asc, NW24800080.asc,  
NW24800100.asc, NW24800120.asc, NW24800140.asc, NW25000040.asc,  
NW25000060.asc, NW25000080.asc, NW25000100.asc, NW25000120.asc,  
NW25000140.asc, NW25200040.asc, NW25200060.asc, NW25200080.asc,  
NW25400040.asc, NW25400060.asc, NW25400080.asc.